

Official (Closed) - Non Sensitive

Official (Closed) - Non Sensitive

Explainable detection of myocardial infarction using deep learning models with Grad-CAM technique on ECG signals

V Jahmunah¹, E.Y.K. Ng¹, Ru- San Tan², Shu Lih Oh³, U Rajendra Acharya^{3,4,5,6,7*}

¹ Department of Mechanical and Aerospace Engineering, Nanyang Technological University.

² National Heart Centre, Singapore.

³ School of Engineering, Ngee Ann Polytechnic, Singapore

⁴ Biomedical Engineering, School of Social Science and Technology, Singapore University of Social Sciences, Singapore

⁵ International Research Organization for Advanced Science and Technology (IROAST), Kumamoto University, Kumamoto, Japan.

⁶ Department Bioinformatics and Medical Engineering, Asia University, Taiwan.

⁷ School of Management and Enterprise, University of Southern Queensland, Australia

Corresponding Address: School of Mechanical and Aerospace Engineering, Nanyang Technological University, Singapore 639798.

*Email Address: aru@np.edu.sg

ABSTRACT

Myocardial infarct (MI) accounts for a high number of deaths globally. In acute MI, accurate electrocardiography (ECG) is important for timely diagnosis and intervention in the emergency setting. Machine learning is increasingly being explored for automated computer-aided ECG diagnosis of cardiovascular diseases. In this study, we have developed DenseNet and CNN models for classification of healthy subjects and patients with ten classes of MI based on the location of myocardial involvement. ECG signals from the Physikalisch-Technische Bundesanstalt database were pre-processed, and the ECG beats were extracted using an R peak detection algorithm. The beats were then fed to the two models separately. While both models attained high classification accuracies (more than 95%), DenseNet is the preferred model for the classification task due to its low computational complexity and higher classification accuracy than the CNN

model due to feature reusability. An enhanced class activation mapping (CAM) technique called Grad-CAM was subsequently applied to the outputs of both models to enable visualization of the specific ECG leads and portions of ECG waves that were most influential for the predictive decisions made by the models for the 11 classes. It was observed that Lead V4 was the most activated lead in both the DenseNet and CNN models. Furthermore, this study has also established the different leads and parts of the signal that get activated for each class. This is the first study to report features that influenced the classification decisions of deep models for multiclass classification of MI and healthy ECGs. Hence this study is crucial and contributes significantly to the medical field as with some level of visible explainability of the inner workings of the models, the developed DenseNet and CNN models may garner needed clinical acceptance and have the potential to be implemented for ECG triage of MI diagnosis in hospitals and remote out-of-hospital settings.

Keywords –Myocardial infarction, DenseNet model, explainable artificial intelligence, Grad-CAM, deep learning

1. Introduction

Cardiovascular diseases cause 17.9 million deaths annually [1], which is projected to increase to 23.6 million by 2030 with a growing prevalence of obesity, diabetes, and other risk factors [2]. Among cardiovascular diseases, myocardial infarction (MI) accounts for the largest percentage of deaths [3]. MI occurs due to acute thrombotic occlusion of the coronary artery at the site of atherosclerotic disease, which results in heart muscle necrosis [3]. Clinical manifestations of MI include chest pain and shortness of breath [4], but symptoms and physical signs are neither sensitive nor specific for MI diagnosis. Electrocardiogram (ECG) and cardiac enzymes are the cornerstones of early diagnosis in the acute setting that crucially decide the need for emergency intervention for potentially life-saving revascularization of the culprit coronary artery. However, cardiac enzymes may not be elevated early in the course of acute MI [5]. As such, ECG signals, which reflect the electrical activity of the heart and will demonstrate instantaneous morphological changes during MI-induced myocardial ischemia [6], constitute the first-line investigation in the emergent situation [7].

Manual ECG interpretation demands domain knowledge and is subject to interobserver variability. Medical expertise may not be physically available in certain circumstances, e.g., para-

medic first responders in remote geographical locations. This has motivated growing research into artificial intelligence (AI)-enabled computer-aided diagnosis for MI using ECG signals [5] [6]. Machine learning can be generally divided into feature engineering and deep learning approaches. The former requires high-level design input into handcrafted features. In contrast, feature extraction and selection processes are completely automated in the latter, which has gained popularity due to its expedience, robust performance, and ability to train large datasets [6].

2. Problem statement and gap in existing work

The major disadvantage of deep models is the lack of explainability: the internal workings and mechanisms of the models cannot be explained, and the rationale behind the predictions are not understandable [8]. This is also a significant gap in the existing literature, wherein none of the authors who developed deep models for MI detection in recent studies had explained how the models made the predictions. Furthermore, the lack of explanation of the mechanisms of these models also poses a challenge as clinicians lose confidence in using deep models in clinical settings to aid in diagnostic decisions. Thus, to address this problem and bridge the gap in existing literature, we have developed and compared the performance of two deep learning models for the classification of MI. After that, we applied a class activation mapping (CAM) visualization technique called Grad-CAM to the model outputs to depict the detailed locations on the ECG signals that had influenced the prediction.

3. Deep learning models

AI-based machine learning has become a valuable diagnostic and predictive tool for diverse diseases, including cardiovascular diseases [9], which sometimes outperforms medical experts [9]. Deep learning can identify complex patterns within training data and are more scalable than conventional shallow learning models. In addition, the size of the network or data can be increased, which enhances predictive accuracy [10]. As feature extraction and selection are fully automated and dispense with handcrafted feature engineering, deep learning has gained popularity due to its expedience and scalability. Deep learning models are being explored widely in various domains, including in cardiological emergencies where the timely identification of ECG signal abnormality is imperative for patient management [10].

Convolutional neural network (CNN) models are commonly used to extract informative features from ECG waveforms. Applications include QRS wave and ST-segment detection for arrhythmia classification [11] and other diagnostic purposes, such as coronary artery disease, myocardial infarction, and congestive heart failure [12], as well as hypertension [13]. Dense convolutional neural network (DenseNet) is a form of CNN network, where enhanced information flow and gradients throughout the network render the network training seamless. Additionally, DenseNet supports feature reuse and bolsters feature propagation, which significantly reduces the number of parameters in the network. Hence, we chose to develop this study's CNN and DenseNet models for MI classification.

4. Data used

The ECGs used in this study were downloaded from the open-access Physikalisch-Technische Bundesanstalt (PTB) database [14]. This database comprises ECG signals from 290 participants from the healthy and different abnormal classes. The participants comprised 209 men and 81 women, whose ages range between 17 and 87 years. However, we used ECG signals from the healthy and MI class for our study.

Our study dataset comprised simultaneous 12-lead ECG signals of 148 MI patients (divided into ten classes by the location of the MI) and 52 healthy control subjects.

5. Methodology

5.1 Pre-processing of signals

All ECG signals had been digitally sampled at 1000 Hz with 16-bit resolution over a range of \pm 16.384 mV at the source [14]. We performed noise and baseline wander removal on the signals using Daubechies 6 (Db6) wavelet function [15]. The decomposition was performed up to four levels. The lower frequency coefficients were disregarded to remove the baseline wander.

5.2 R peak detection for beat selection

After de-noising, individual beats on the ECG signal were selected by using Pan-Tompkin's algorithm [16] to detect the peak of the R wave in every QRS complex. Upon identification of the R peak, the corresponding ECG beat was extracted by selecting 250 and 400 samples to the left and right, respectively, of the R-peak to construct a 651-sample segment. As the ECG signals

had been acquired simultaneously, each beat would generate twelve 651-sample segments. The ECG segments (12 per beat) were then fed to the deep CNN and DenseNet models. [Table 1](#) details the number of ECG beats extracted for the healthy and ten MI classes. [Figure 1](#) shows the output of the pre-processing techniques, using a healthy signal as an example.

Table 1. Number of beats extracted per class

Class type	Number of beats/records
Healthy	10,304
Inferior	10,215
Inferior lateral	5,822
Inferior posterior	48
Inferior posterior lateral	2,495
Anterior	4,659
Anterior lateral	6,142
Anterior septal	7,976
Lateral	459
Posterior	459
Posterior lateral	655
	Total: 49,234

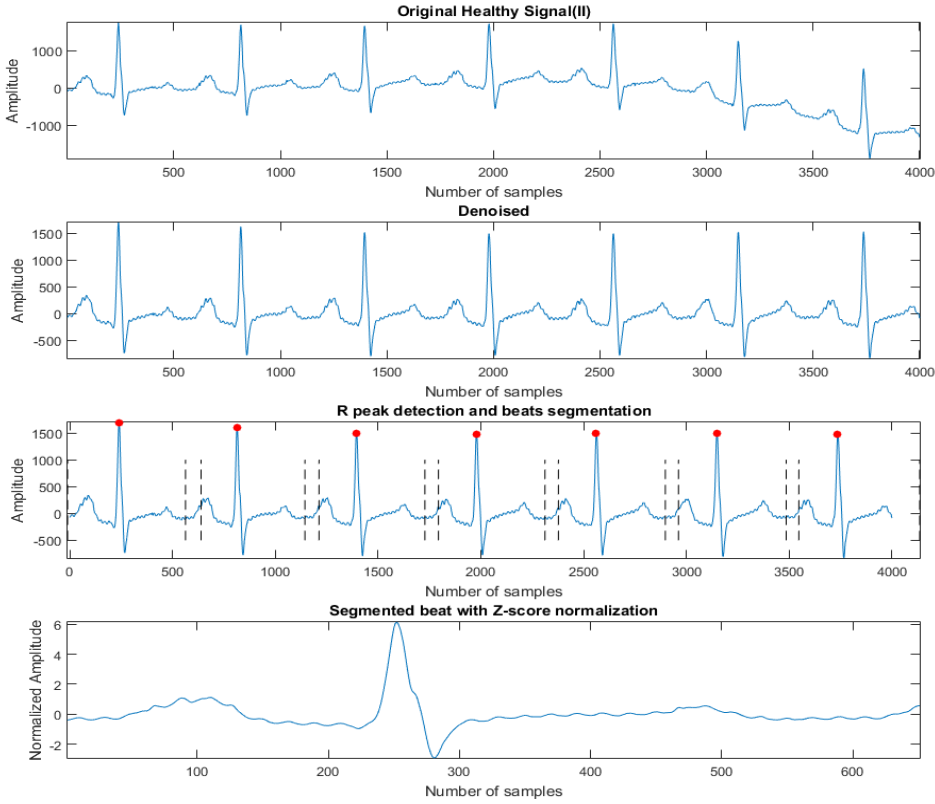


Figure 1: Output of the pre-processing techniques using a healthy signal as an example.

5.3 CNN and DenseNet models

A typical CNN model comprises three main layers: convolution, pooling, and fully connected layers. Filters in the convolution layer are trained to extract distinct features from the input data to form feature maps. The latter is, in turn, fed to the next convolution layer, and this process is repeated deeper into the network, where progressively more complex features are extracted [17]. Pooling layers reduce the dimensionality of the feature maps and prevent the overfitting of the network. Our CNN model was trained using a backpropagation algorithm [18], where weight coefficients in the layers were updated based on the stochastic gradient descent [19]. The fully connected layer at the end of the CNN then classified the data based on representing the extracted features in the penultimate layer.

In contrast to the sequential architecture of the CNN, every layer in a DenseNet is connected to every other layer in the network in a feed-forward manner [20]. The DenseNet forms a dense

connectivity pattern with $\frac{L(L+1)}{2}$ connections in a network with L layers [20], whereas a typical CNN model with L layers would only have L connections (one between two layers). A typical DenseNet contains dense blocks and transition layers. The former comprises many convolution blocks, each with an identical number of output channels. During the forward propagation, feature maps learned by the different layers are concatenated, enabling feature reuse and causing variation in the input of succeeding layers, thereby improving efficacy [20]. Transition layers perform convolution and pooling operations, which aid in reducing the number of channels and complexity of the network. We added a bottleneck layer to our DenseNet model to limit the number of feature maps and reduce the computational complexity of the model [20]. The classification was then made based on all the feature maps in the network. [Figure 2](#) illustrates the study workflow.



Figure 2: Workflow of the proposed methodology.

Developed DenseNet model

We first developed a DenseNet model for one-lead ECG signal classification with the following hyperparameters: batch size 50; 60 epochs; learning rate 0.0001; and Adam optimizer betas (0.9, 0.999) [21]. Each layer in the dense blocks received feature map inputs from all previous layers, which would then undergo a series of operations: batch normalization to standardize the outputs of the previous layers; rectified linear unit activation to introduce nonlinearity and enable the model to learn faster and perform better, and 3 x 1 one-dimensional (1D) convolution. Accordingly, the l th layer obtained feature maps of all previous layers, x_0, \dots, x_{l-1} as input data as governed by the equation below:

$$x_l = H_l, (|x_0, x_1, \dots, x_{l-1}|) \quad (1)$$

where $[x_0, x_1, \dots, x_{l-1}]$ refers to the concatenation of all feature maps formed in $0, \dots, l-1$. Transition layers were then added between the dense blocks that comprised a batch normalization layer and a 1×1 convolution, which helped reduce the feature maps and improve model compactness, followed by a 2×1 1D average pooling layer helped reduce the size of the feature maps. To control the amount of new information that each layer would contribute to the global state, the growth rate was set at $k = 8$ for the network. A 1×1 convolution was introduced as the bottleneck layer before each 3×1 1D convolution, compared to the usual 3×3 convolution used in the dense blocks, to reduce the number of feature maps, thereby enhancing the network's computational efficiency. The weight map [22] from the weighted loss function was implemented in the network to balance the data used in this study. Between the convolution and pooling layers, the ReLU (rectified linear unit) activation function was used to introduce nonlinearity to decrease the computation of the network. The SoftMax activation is used at the output layer, wherein it provides the probability that data belongs to a class. This enables the prediction of results. The same DenseNet model was then developed for all the 12 ECG lead signals for each beat (Table 2). The trainable parameters of the DenseNet and CNN models are 82 355 and 65 843, respectively.

Table 2. DenseNet architecture for 12 ECG leads.

Layers	Input/ Output size	DenseNet		
Dense block	651	1D Convolution (Kernel size: 1)	X 2	
	651	1D Convolution (Kernel size: 3)		
Transition layer	651	1D Convolution (Kernel size: 1)		X 12
	651	1D Average Pooling (Kernel size: 2, Stride: 2)		
Dense block	326	1D Convolution (Kernel size: 1)	X 3	
	326	1D Convolution (Kernel size: 3)		
Transition layer	326	1D Convolution (Kernel size: 1)		
	326	1D Average Pooling (Kernel size: 2, Stride: 2)		
Classification layer	1	Global average pooling		
		Fully connected (11)		

Developed CNN model

The same hyperparameters and layers used to develop the DenseNet model were deployed in CNN model except that the connections were removed to disable concatenation of features for the CNN model. Similar to conventional CNN, our CNN model fed the output of the l th layer to the $(l+1)^{\text{th}}$ layer as directed by the equation below:

$$x_l = H_l (x_l - 1) \quad (2)$$

6. Results

Both models were evaluated using the 10-fold cross-validation, wherein 90% of the entire data was used for training and the remaining data for testing. The training data was further split into 80% for training and 20% for validation of the model, respectively.

The accuracy, specificity, and sensitivity performance matrices were used to evaluate the models. Accuracy, specificity, and sensitivity matrices indicate the correct classifications that were made out of all the classifications, the negative cases out of the total number of original negative cases, and the positive cases out of the total number of original positive cases, respectively. As these are crucial performance matrices, they were used to evaluate the performances of both models. Both DenseNet and CNN models attained good classification results (Tables 3 and 4) with average accuracy rates of 98.9% and 98.5%, respectively. Both models observed the best performance in the inferior posterior, lateral, posterior, and posterior-lateral MI classes.

Table 3. Classification results of DenseNet model.

Class type	Average accuracy (%)	Average specificity (%)	Average sensitivity (%)	Overall accuracy of the model (%)
Normal	98.8	99.3	96.8	98.9
Inferior	96.9	98.7	90.4	
Inferior lateral	98.2	98.8	93.7	
Inferior posterior	99.9	99.9	100	
Inferior posterior	99.4	99.6	95.9	

lateral				
Anterior	98.5	99.2	91.4	
Anterior lateral	98.5	99.0	95.0	
Anterior septal	97.9	98.5	94.9	
Lateral	99.9	99.9	99.3	
Posterior	99.9	99.9	100	
Posterior lateral	99.9	99.9	98.0	

Table 4. Classification results of CNN model.

Class type	Average accuracy (%)	Average specificity (%)	Average sensitivity (%)	Overall accuracy of the model (%)
Normal	98.9	99.4	97.1	98.5
Inferior	95.9	97.3	90.6	
Inferior lateral	97.6	98.5	91.3	
Inferior posterior	99.9	99.9	97.9	
Inferior posterior lateral	98.8	99.0	94.9	
Anterior	98.2	98.9	90.7	
Anterior lateral	97.8	99.0	89.5	
Anterior septal	96.9	98.6	88.5	
Lateral	99.9	99.9	97.8	
Posterior	99.9	99.9	98.0	
Posterior lateral	99.8	99.8	98.0	

7. Discussion

Table 5 summarizes recent studies (in the past five years) that employed deep learning models for classifying MI using the same PTB database with identical numbers of MI (148) and normal (52) subjects. Most authors have employed CNN models in their research. Some studies attained marginally higher classification accuracy rates than our models [23]. Of these, Liu et al. [23], Liu et al. [24], Baloglu et al. [25], Liu et al. [26], Fu et al. [27], and Jafarian et al. [28] used CNN models for the classification task. Compared with the other CNN models, the DenseNet model in our study used the transition and bottleneck layers to reduce the size of feature maps and computational network complexity, allowing the model to predict the classification results more rapidly. Although our DenseNet has more trainable parameters than our CNN model, it is a better model due to its low complexity (usage of 1x1 convolution bottleneck layer instead of 3x3 convolution) and higher classification accuracy (due to feature reuse). With the low compu-

tational complexity of the DenseNet model, it is well elucidated that the computational costs of training and testing the model is reduced. Thus, the model is fit to be used in clinical settings for MI detection. Zhang et al. [29] and Tripathi et al. [30] employed hybrid machine learning and deep learning techniques, which are comparatively more complex and time-consuming. Han et al. [31] used the ResNet model, which has a significantly larger parameter size than DenseNet, as the layers contain trainable weights [20].

Table 5. Summary of recent studies

Publication	Features and methods	Findings/ Results (%)
Acharya [32]	<ul style="list-style-type: none"> • CNN • 10-fold cross-validation Training, testing, validation phases	<u>Without noise:</u> Accuracy: 95.2%
Reasat [33]	<ul style="list-style-type: none"> • Shallow CNN, inception network • Separability index 	Accuracy: 84.5
Liu [23]	<ul style="list-style-type: none"> • Multiple-feature-branch CNN • Patient-specific paradigm • Class-based, patient-specific experiment 	<u>Class-based detection:</u> Accuracy: 99.95%
Liu [34]	<ul style="list-style-type: none"> • Multi-lead CNN • 5-fold cross-validation 	Accuracy: 96%
Lui [35]	<ul style="list-style-type: none"> • CNN • Recurrent neural network classifier, multi-layer perceptron classifier • 10-fold cross-validation 	F1 score: 94.6
Liu [24]	<ul style="list-style-type: none"> • Deep CNN • 3-second ECG segments • 10-fold cross-validation 	<u>Denoised data:</u> Accuracy: 99.3
Zhang [29]	<ul style="list-style-type: none"> • Autoencoder deep model • Tree bag classifier • 10-fold cross-validation 	Accuracy: 99.9
Tripathi [30]	<ul style="list-style-type: none"> • Deep model • Empirical wavelet transform (Fourier-Bessel) • 5-fold cross-validation • Analytical features(statistics) 	Accuracy: 99.7%
Baloglu [25]	<ul style="list-style-type: none"> • Deep CNN • 10 layers 	Accuracy: 99.8
Feng [36]	<ul style="list-style-type: none"> • CNN • Long-short term memory model 	Accuracy: 95.4

	<ul style="list-style-type: none"> • 10-fold cross-validation 	
Han [31]	<ul style="list-style-type: none"> • Residual neural network (multi-lead) • Intra- and inter-patient strategies • 5-fold cross-validation 	<u>Intra-patient scheme:</u> Accuracy: 99.9
Liu [26]	<ul style="list-style-type: none"> • Convolutional bi-directional recurrent neural network (Multiple-feature-branch) • Mask optimisation • 5-fold cross-validation (Class-based, subject-based) 	<u>Class-based method:</u> Accuracy: 99.9
Fu [27]	<ul style="list-style-type: none"> • Multi-lead mechanism coupled with CNN and bidirectional gated recurrent unit • Temporal features, spatial features 	<u>Intra-patient performance:</u> Accuracy: 99.9
Jafarian [28]	<ul style="list-style-type: none"> • Shallow neural network • End to end residual deep CNN (dilated convolutions) • Principal component analysis • K-fold cross-validation 	<u>End to end convolutional neural network:</u> Accuracy: 100
Manimekalai [37]	<ul style="list-style-type: none"> • CNN + long short-term memory model 	Accuracy: 88.9
Jian [38]	<ul style="list-style-type: none"> • CNN • Multi-lead features-concatenate narrow network, multi-scale features concatenate network • 5-fold cross-validation 	<u>Multi-lead features-concatenate narrow network:</u> Accuracy: 95.8
Current study	<ul style="list-style-type: none"> • DenseNet • CNN • 10-fold cross-validation 	<u>DenseNet model:</u> Average accuracy rate: 98.9

Figure 3 depicts the accuracy plots of the DenseNet and CNN models. While both models learned the data well and trained well over the 60 epochs, the DenseNet model converged better due possibly to the normalizing effect of the dense layers, which reduced the overfitting of the model [20]. Corroborating the good performance of the models, misclassification rates for all classes were very low, as demonstrated in the confusion matrices of the DenseNet and CNN models (Figure 4).

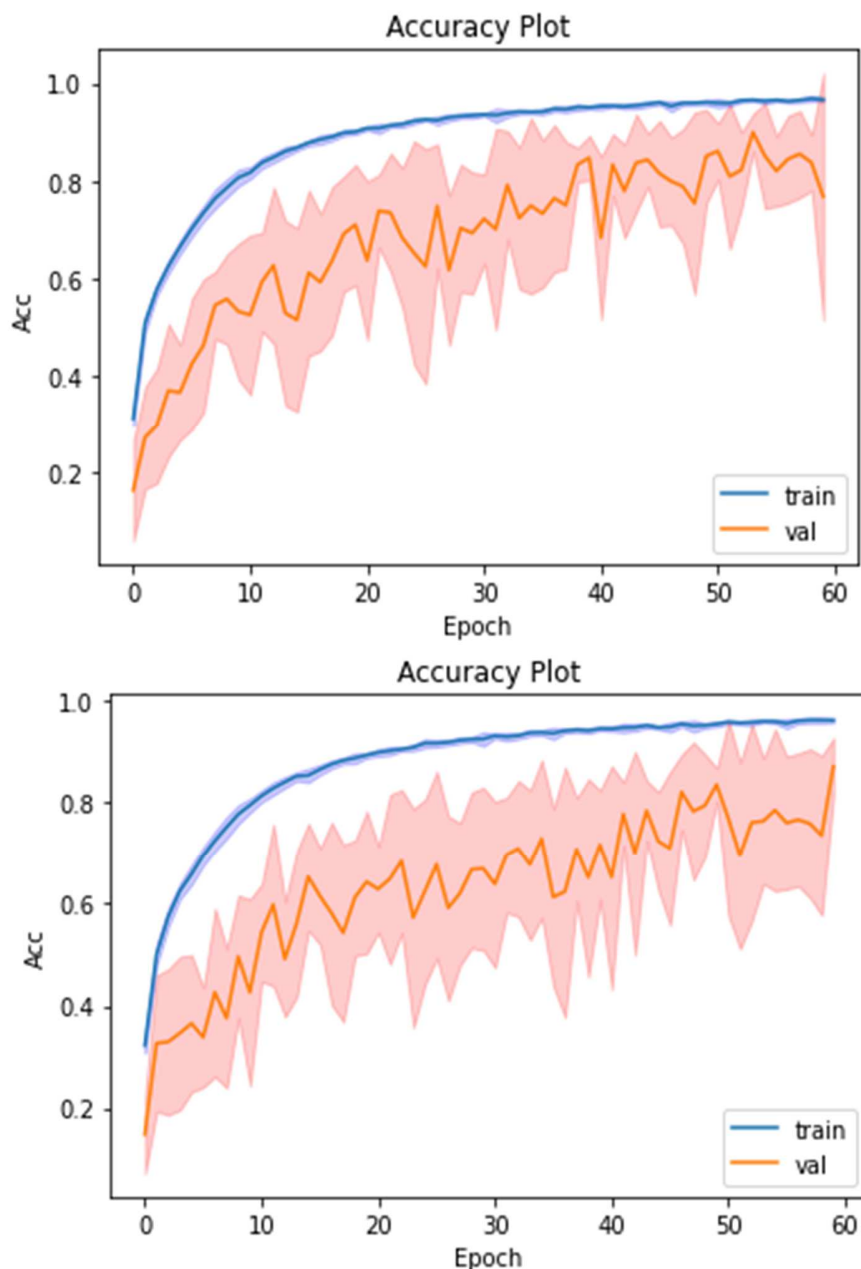
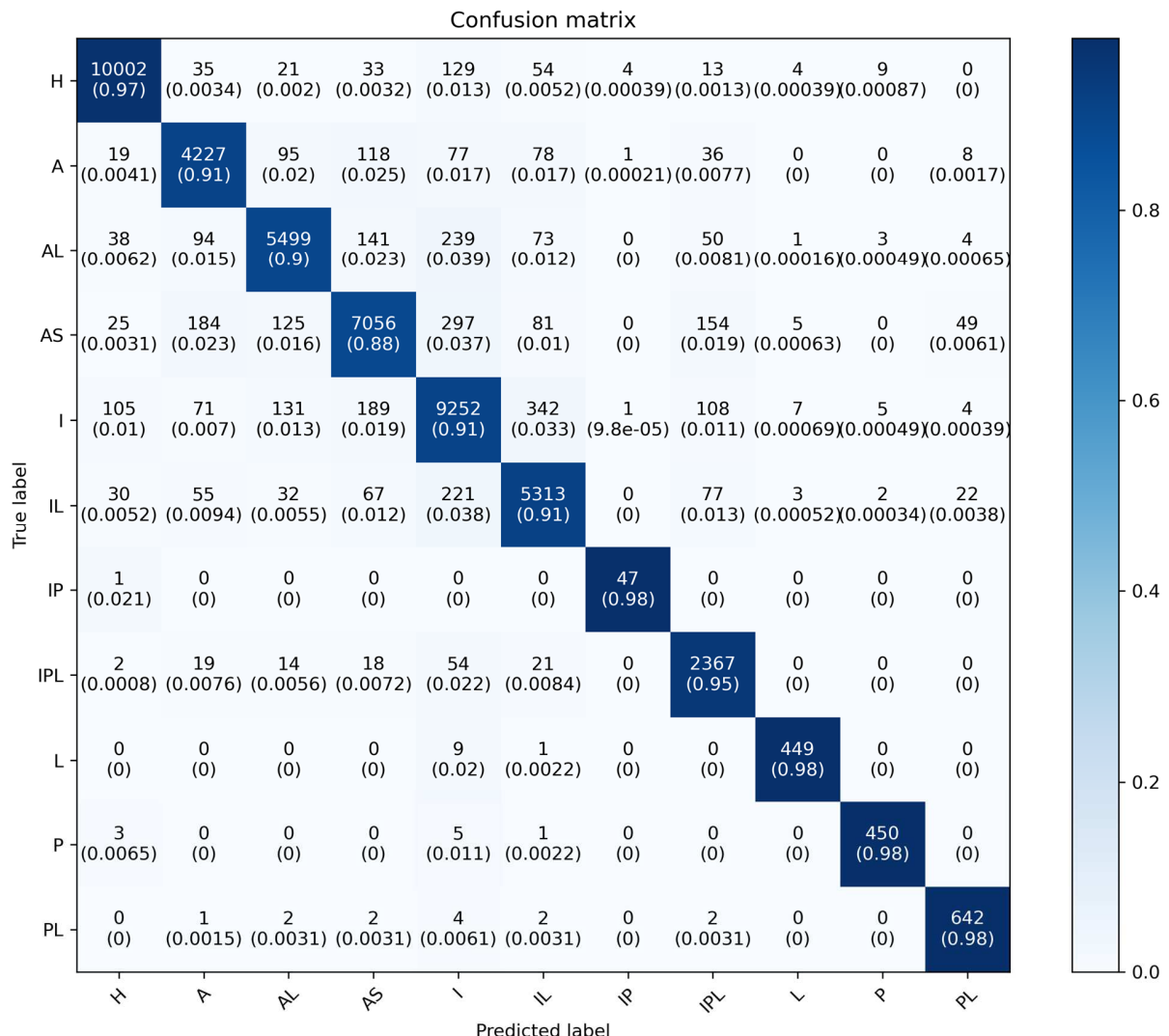
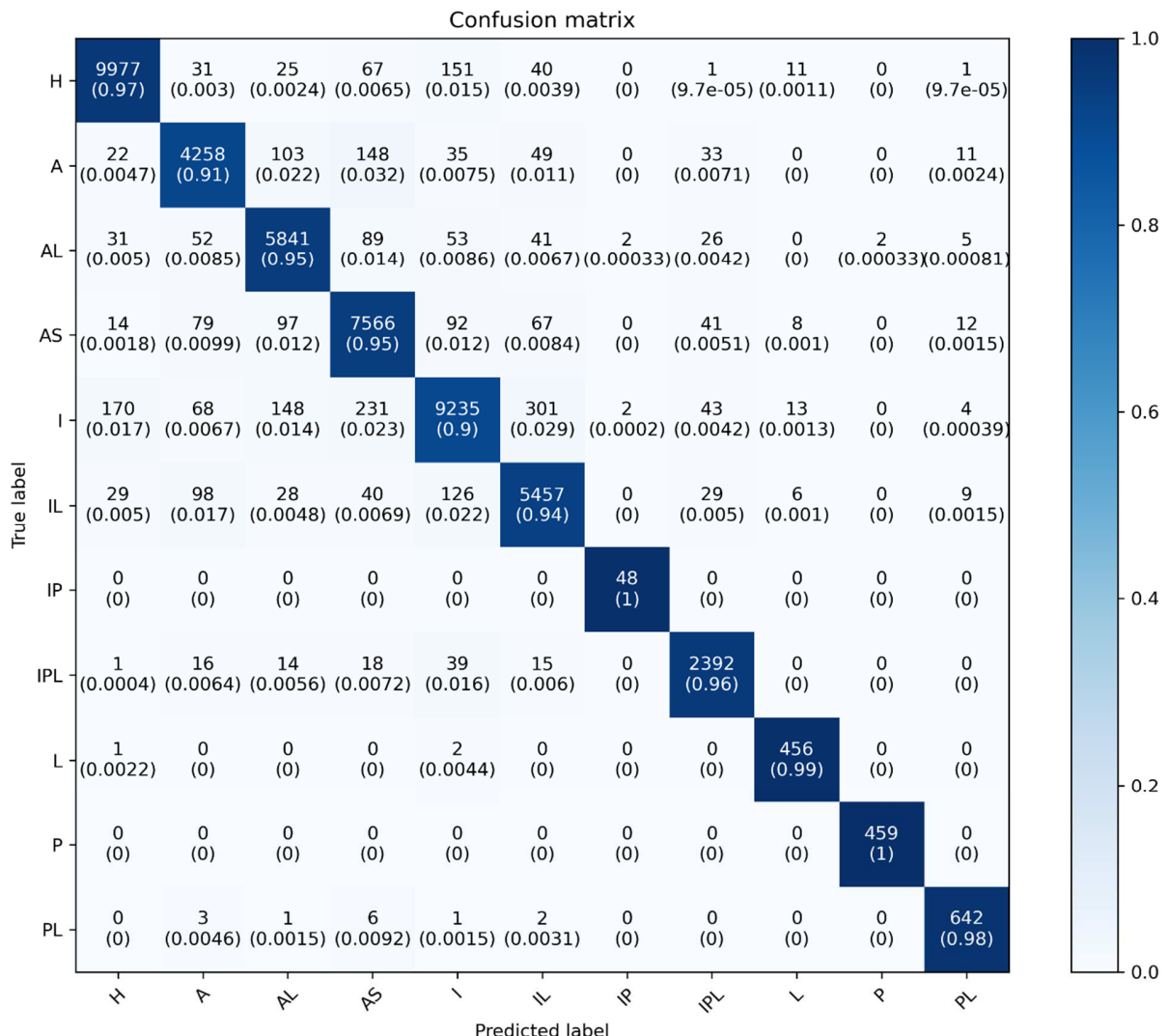


Figure 3. Accuracy plots of DenseNet model (top) and CNN model (bottom).

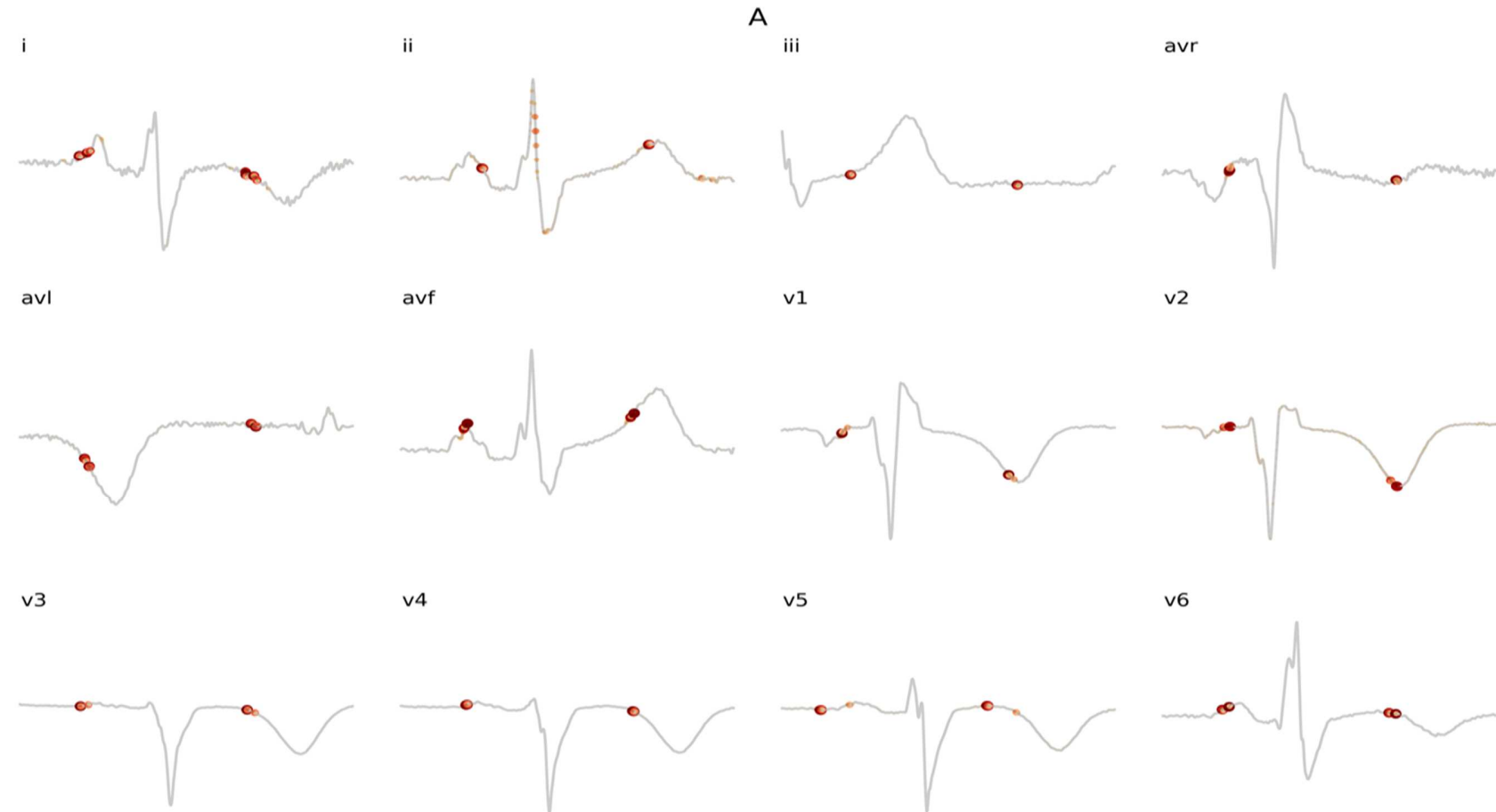


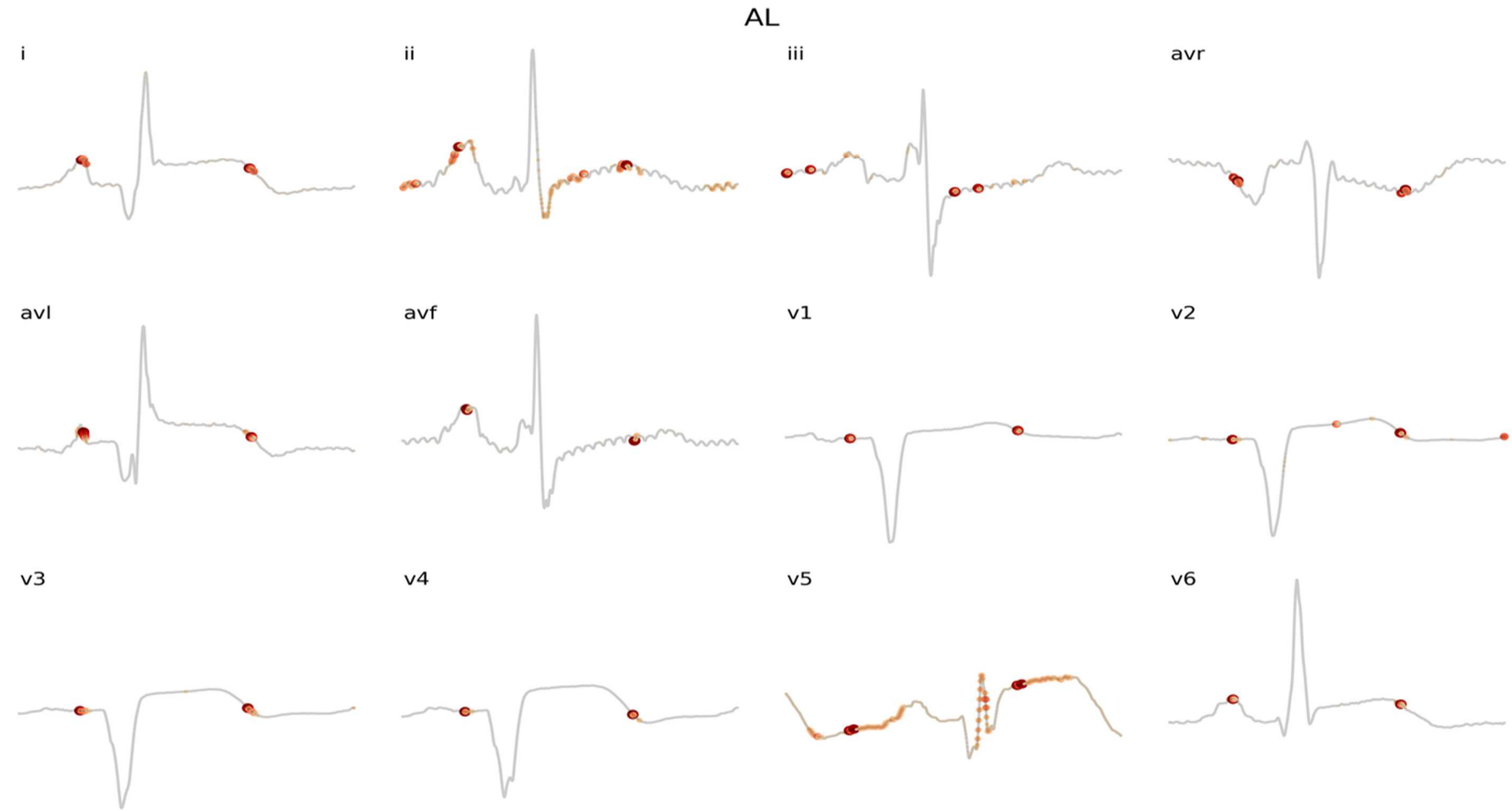
**Figure 4. Confusion matrices of DenseNet model (top) and CNN model (bottom).**

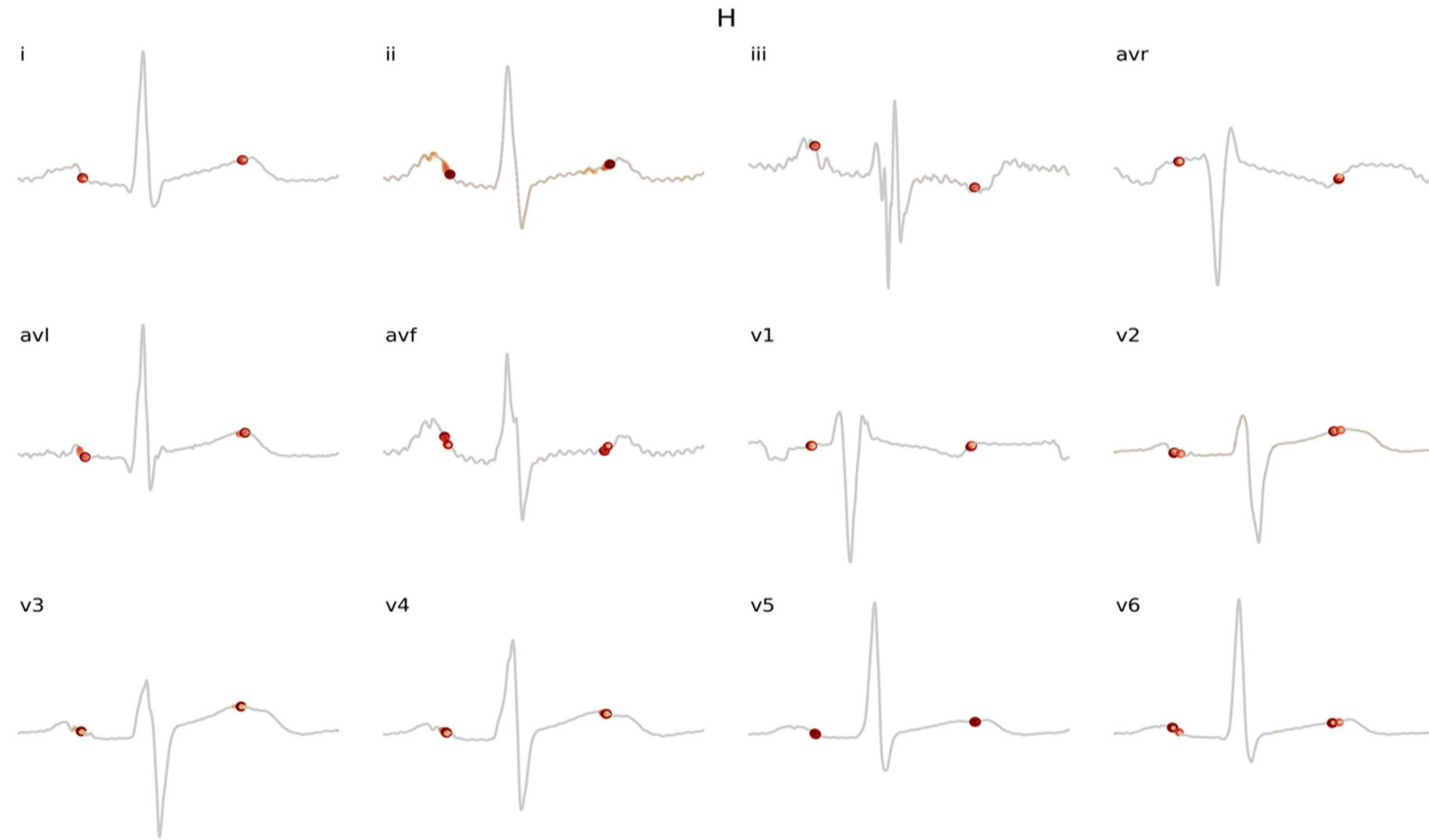
Explainable AI using Grad-CAM technique

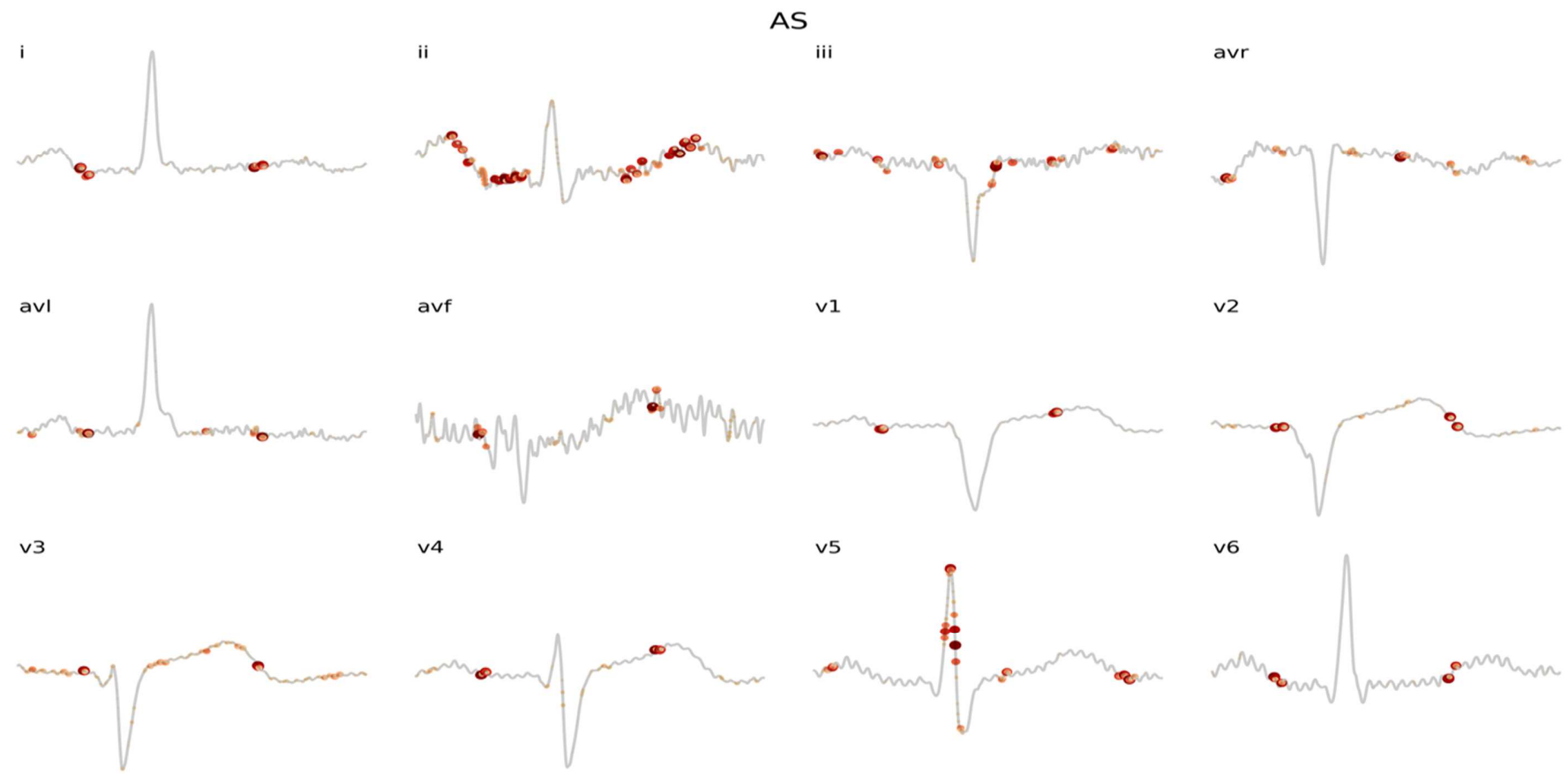
Despite the good classification performance of deep learning models, they remain underutilized as clinicians distrust their black-box nature and cannot accept the undecipherable basis on which these models make predictions that concern patients' health [39] [40]. In response, some authors have used CAM to envisage how predictions are made in CNN models. Kim et al [40] employed the Grad-Cam technique, an enhanced version of CAM, for arrhythmia classification using the DenseNet model. Grad-CAM allows visualization of any chosen layer in the model as

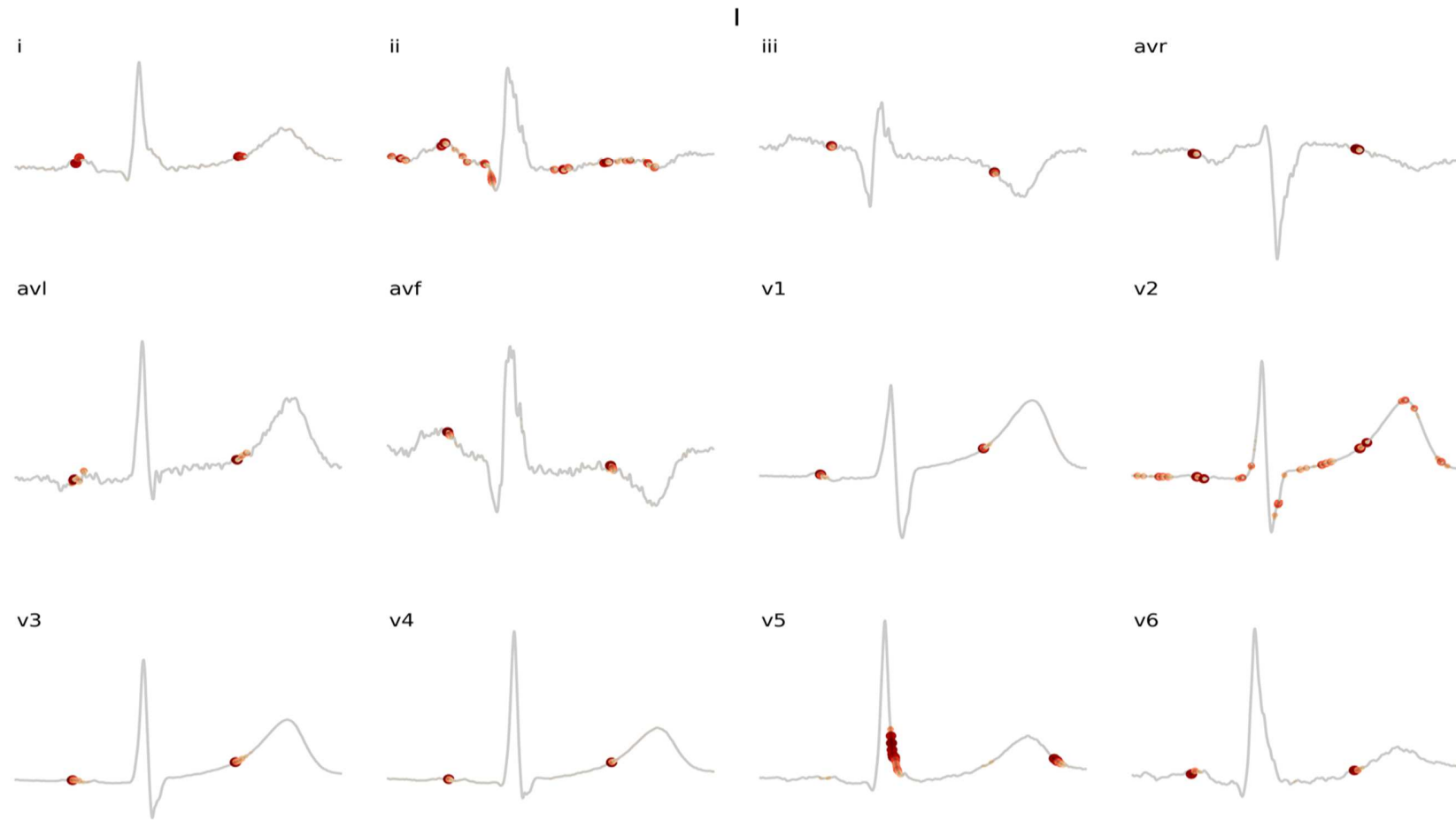
well as scrutiny of every feature map layer, which are necessary for understanding how input values influence model classification [40]. Inspired by this work, we applied Grad-CAM to the output of our models. Figure 4 and 5 depict activation maps generated by Grad-CAM overlaid on example ECG beats of the different MI classes in the DenseNet and CNN models, respectively. Figure 7 shows the heat map of individual lead activations for all the MI classes in the DenseNet and CNN models.

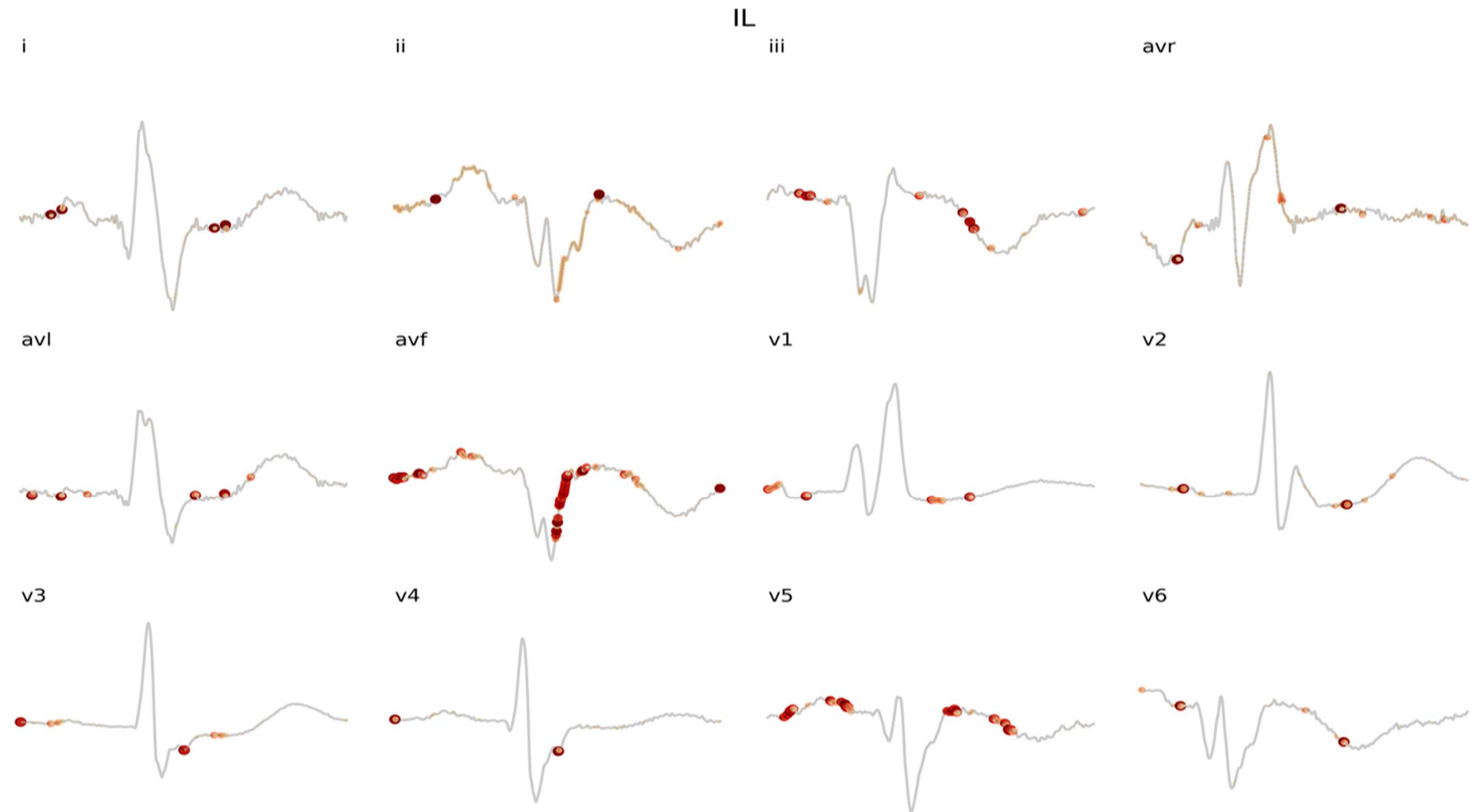


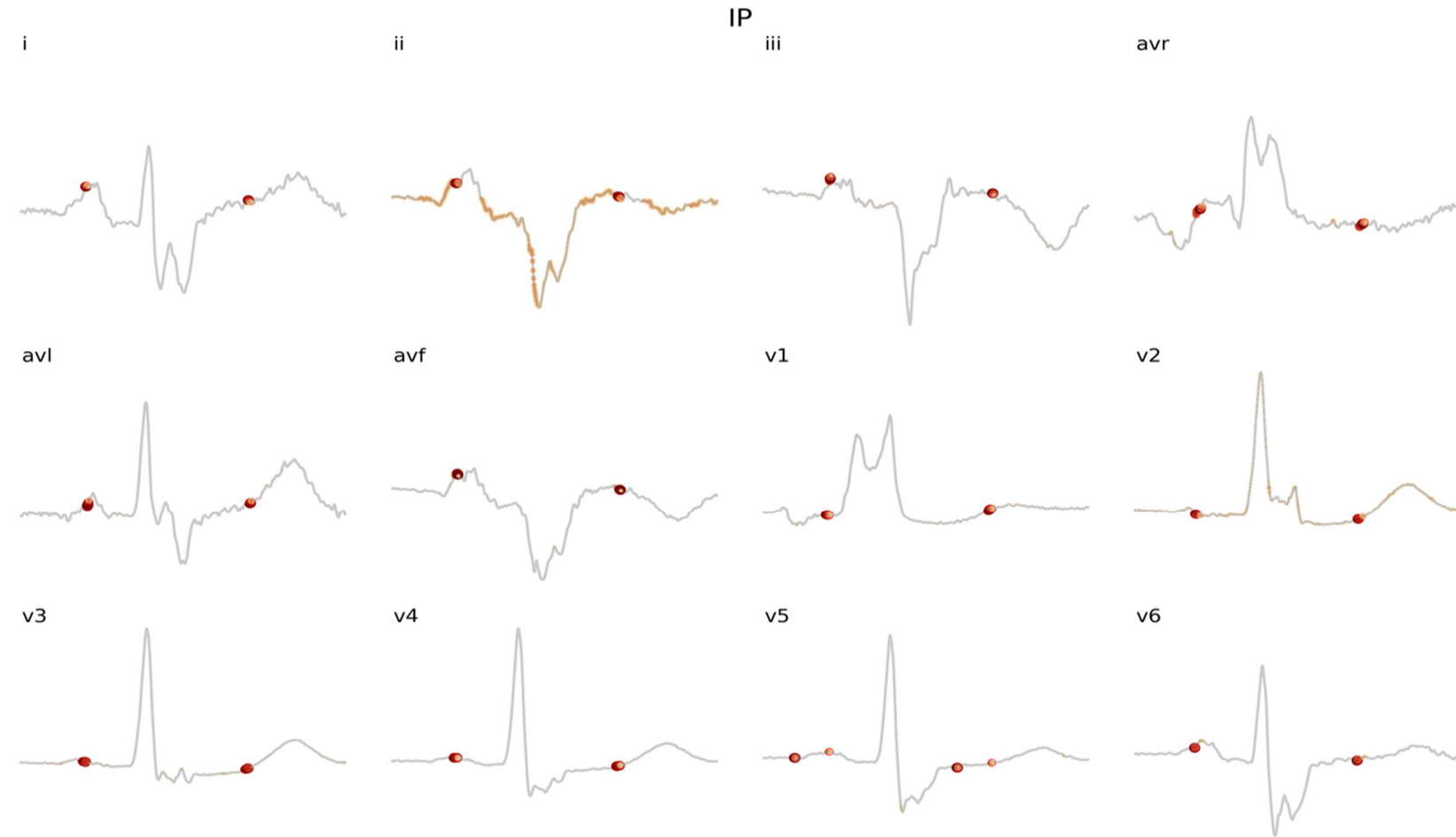


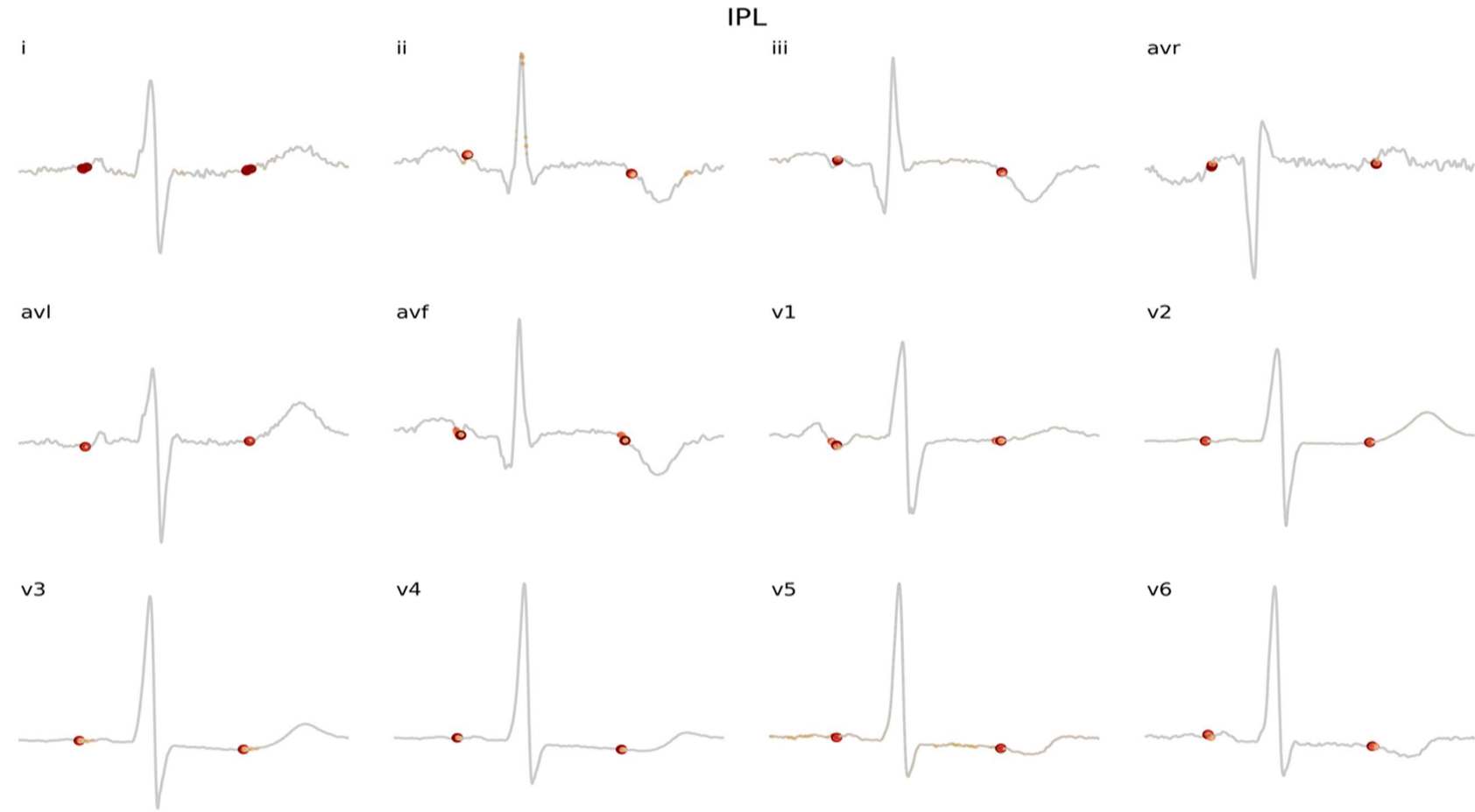


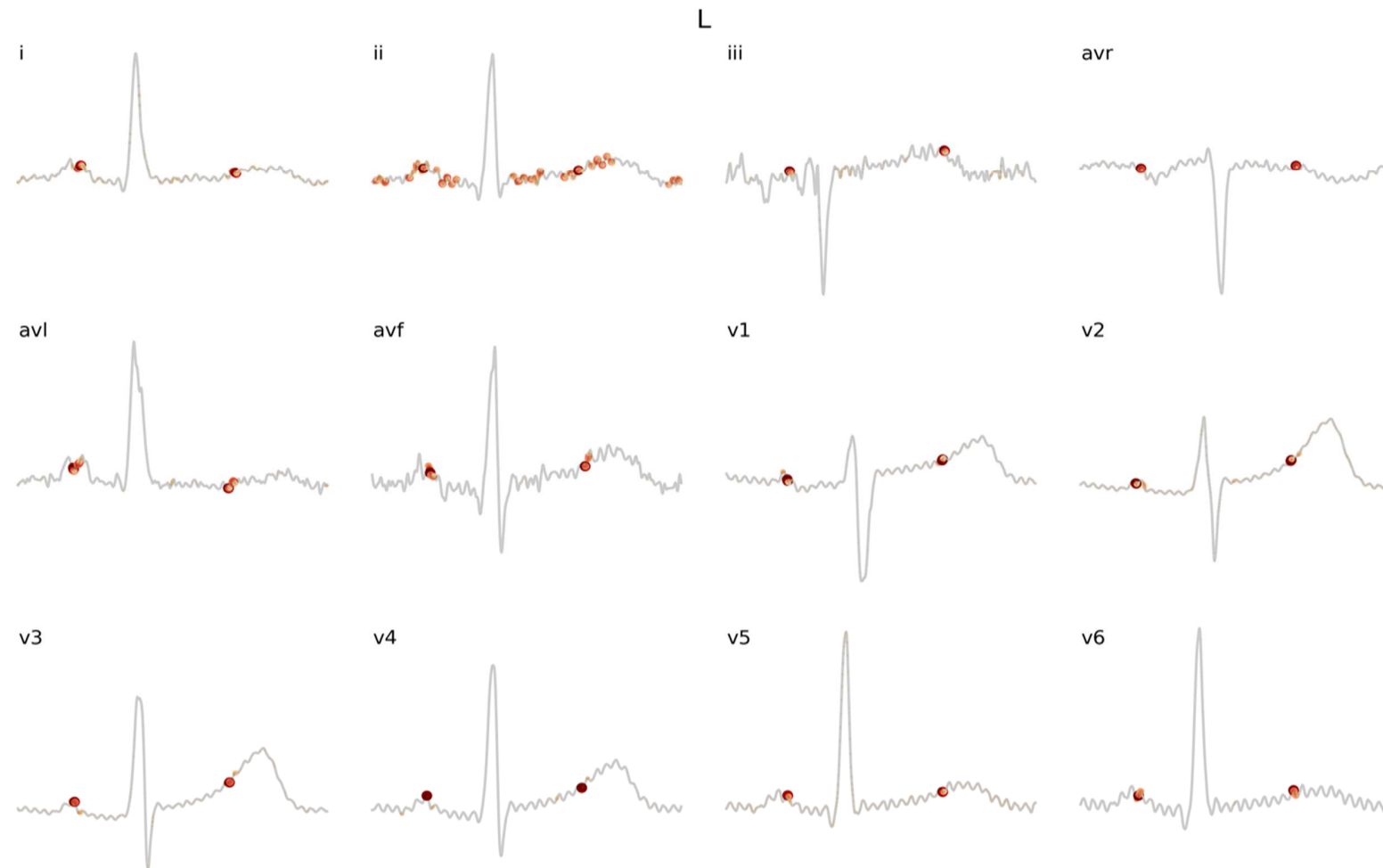


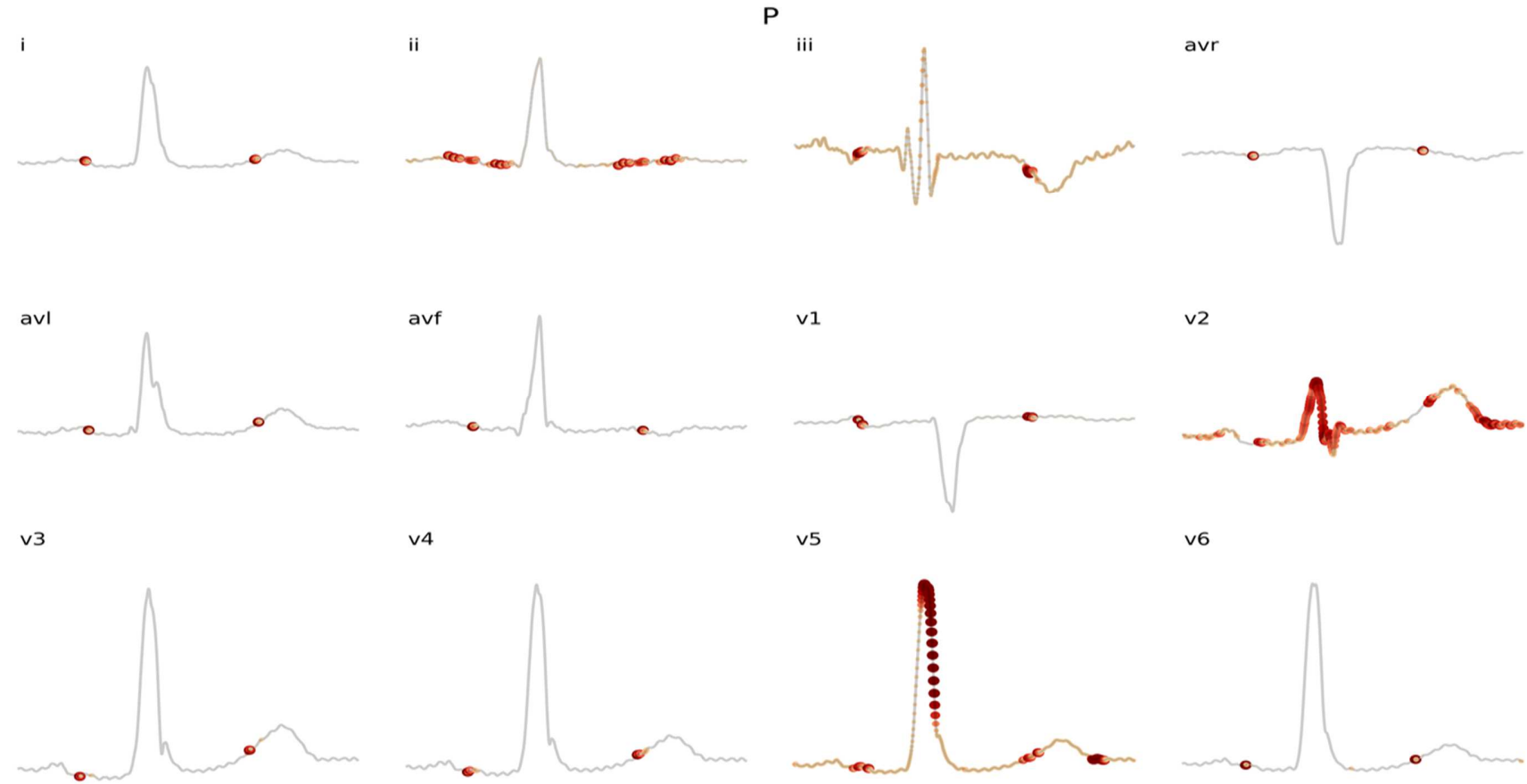












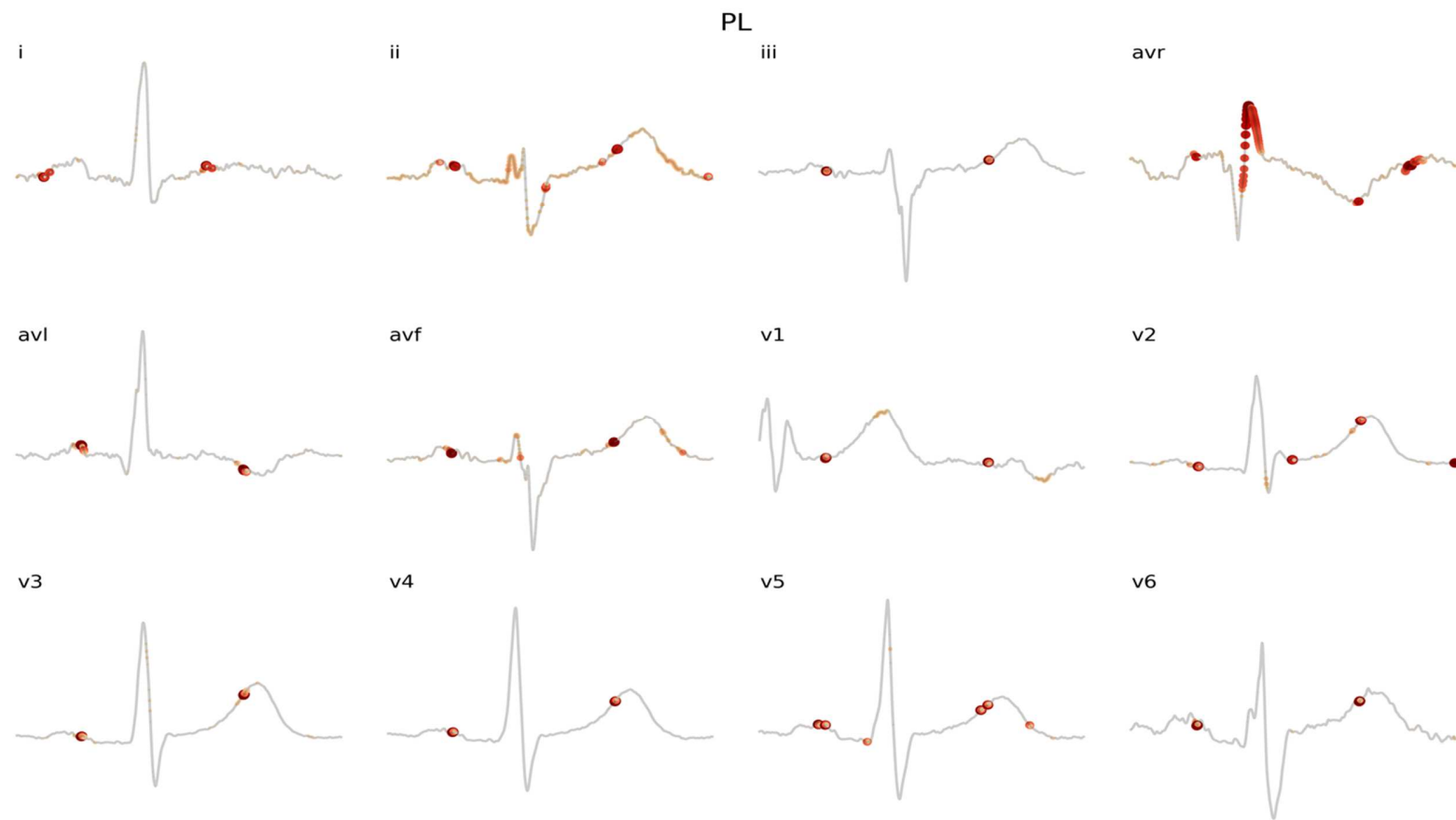
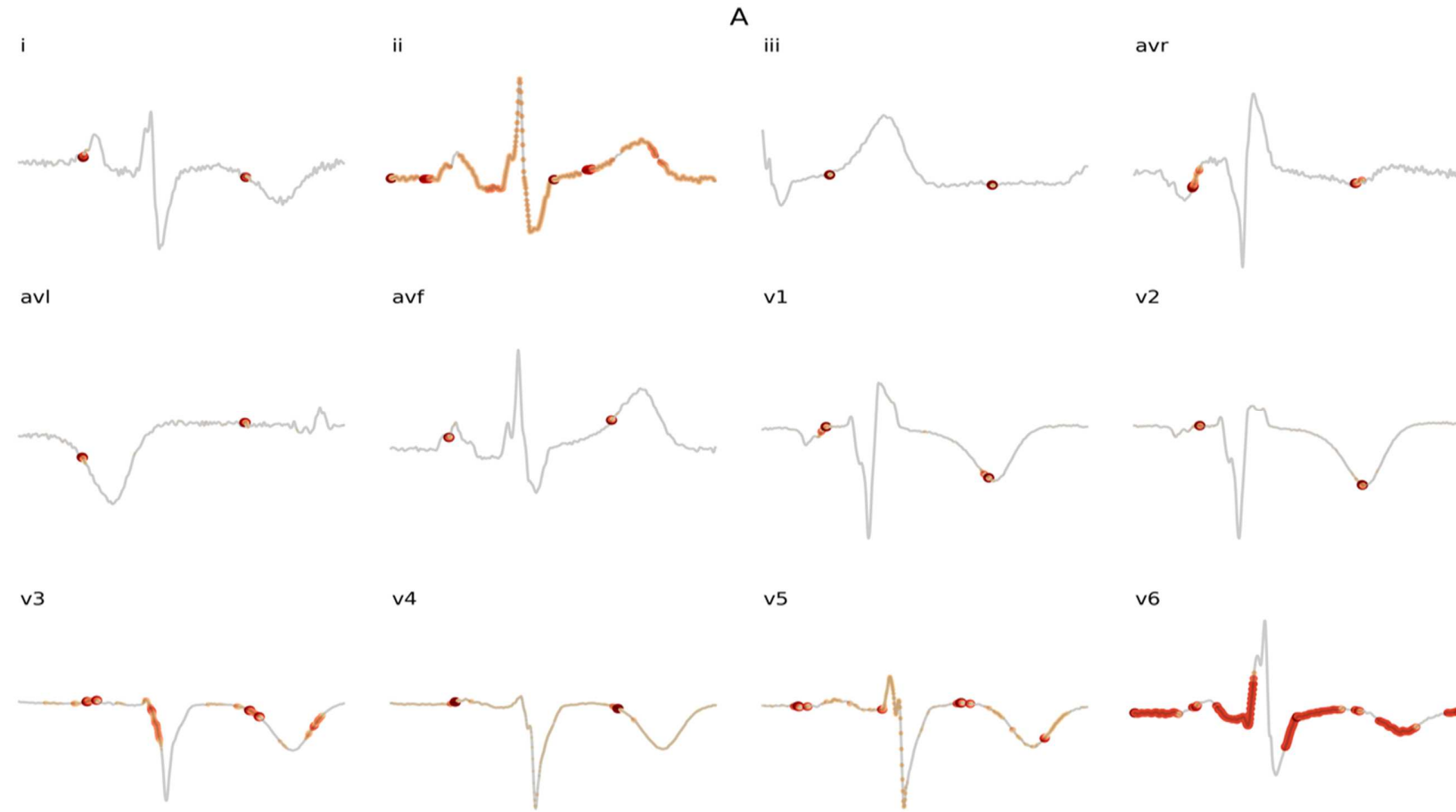
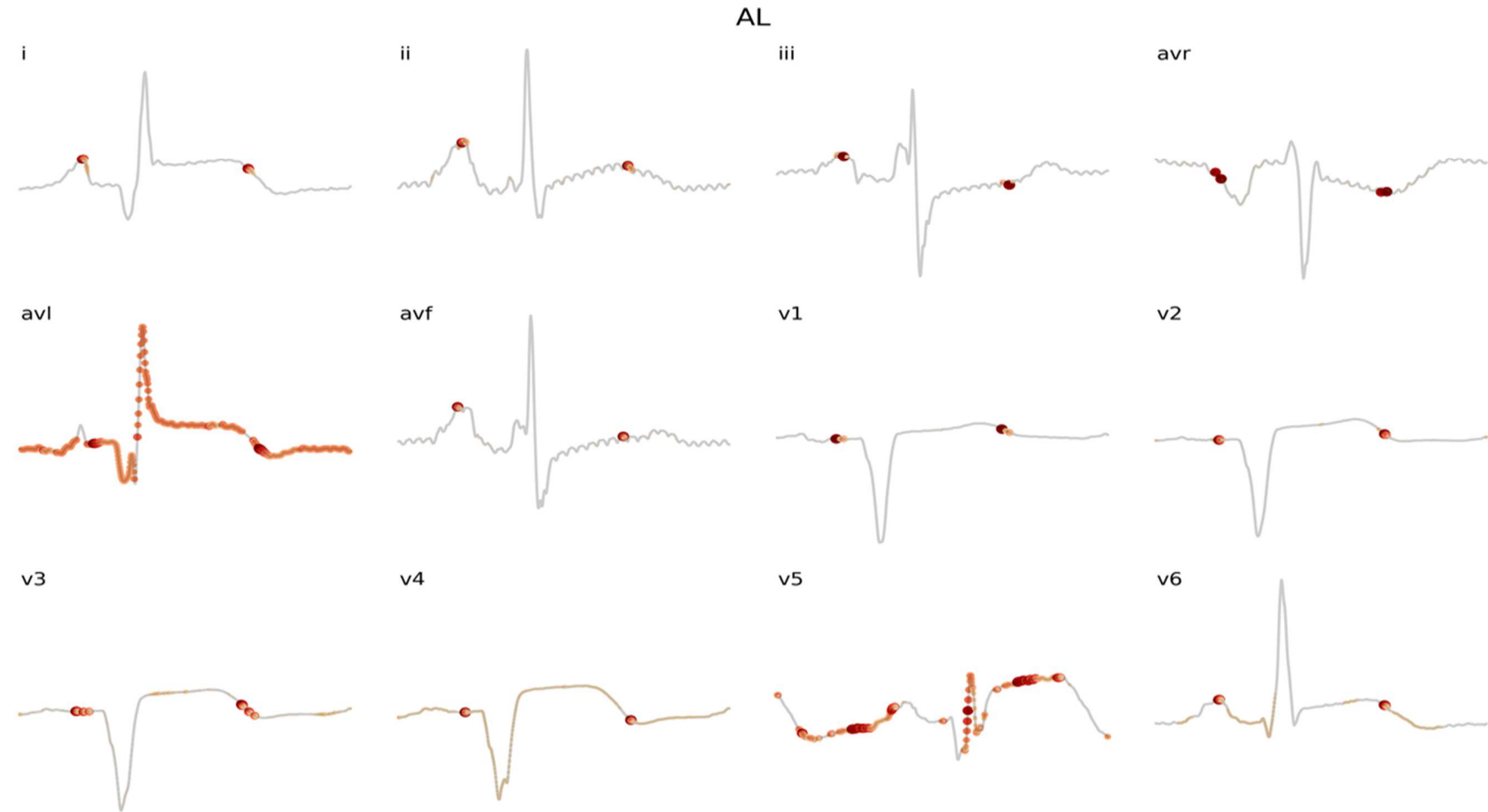
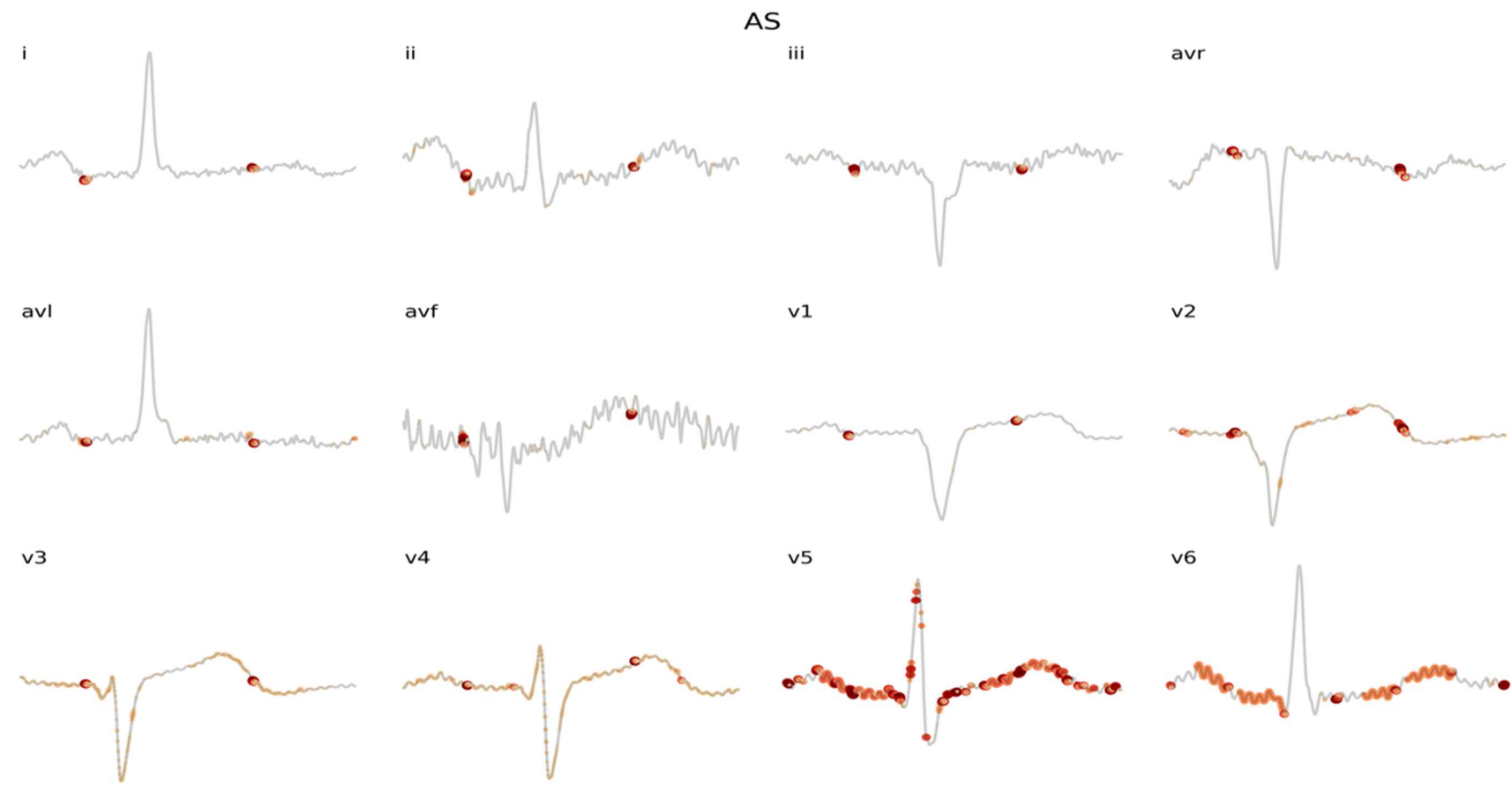
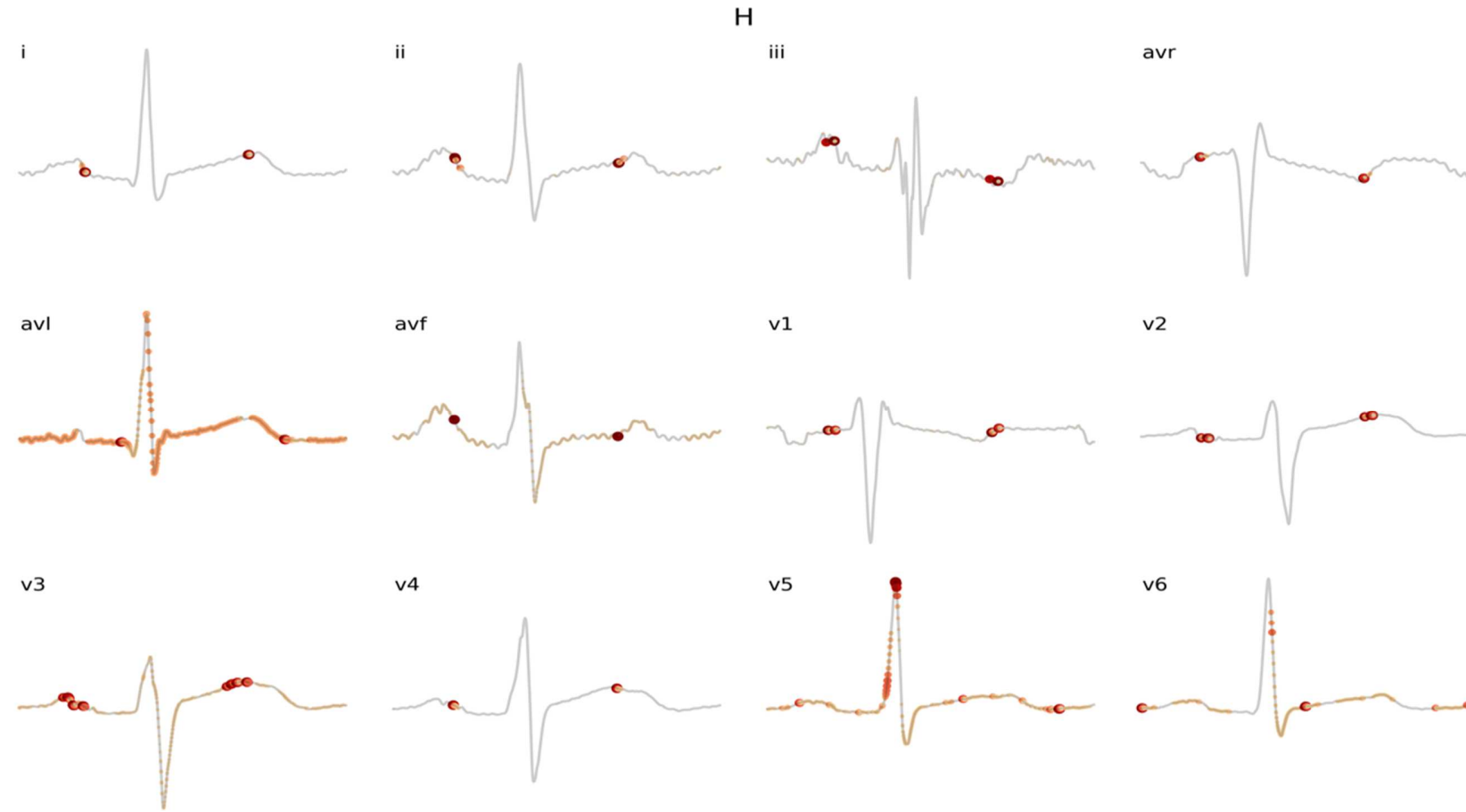


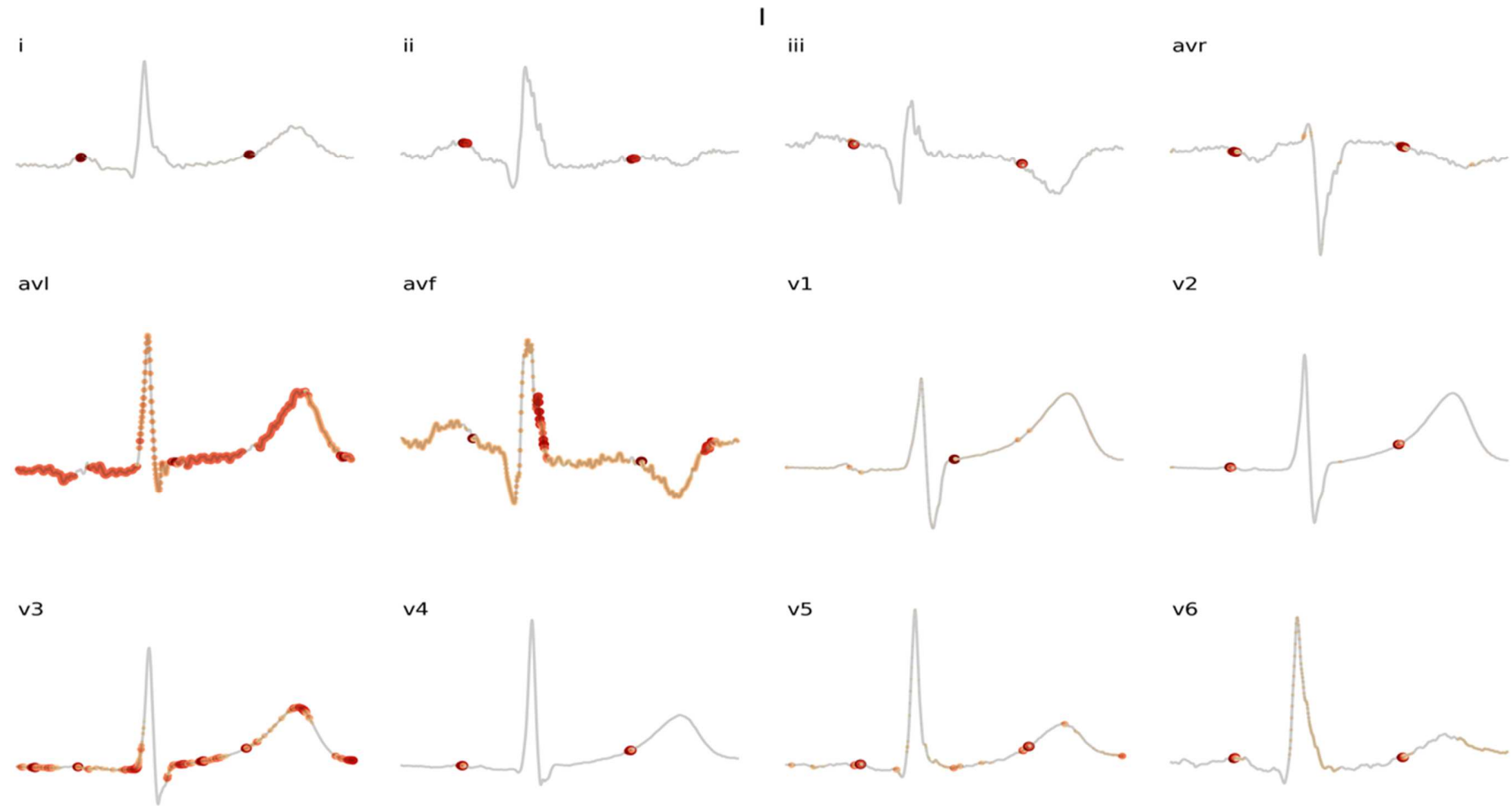
Figure 5. Activation maps of each myocardial infarction class obtained from the Grad-CAM technique (output from DenseNet model).

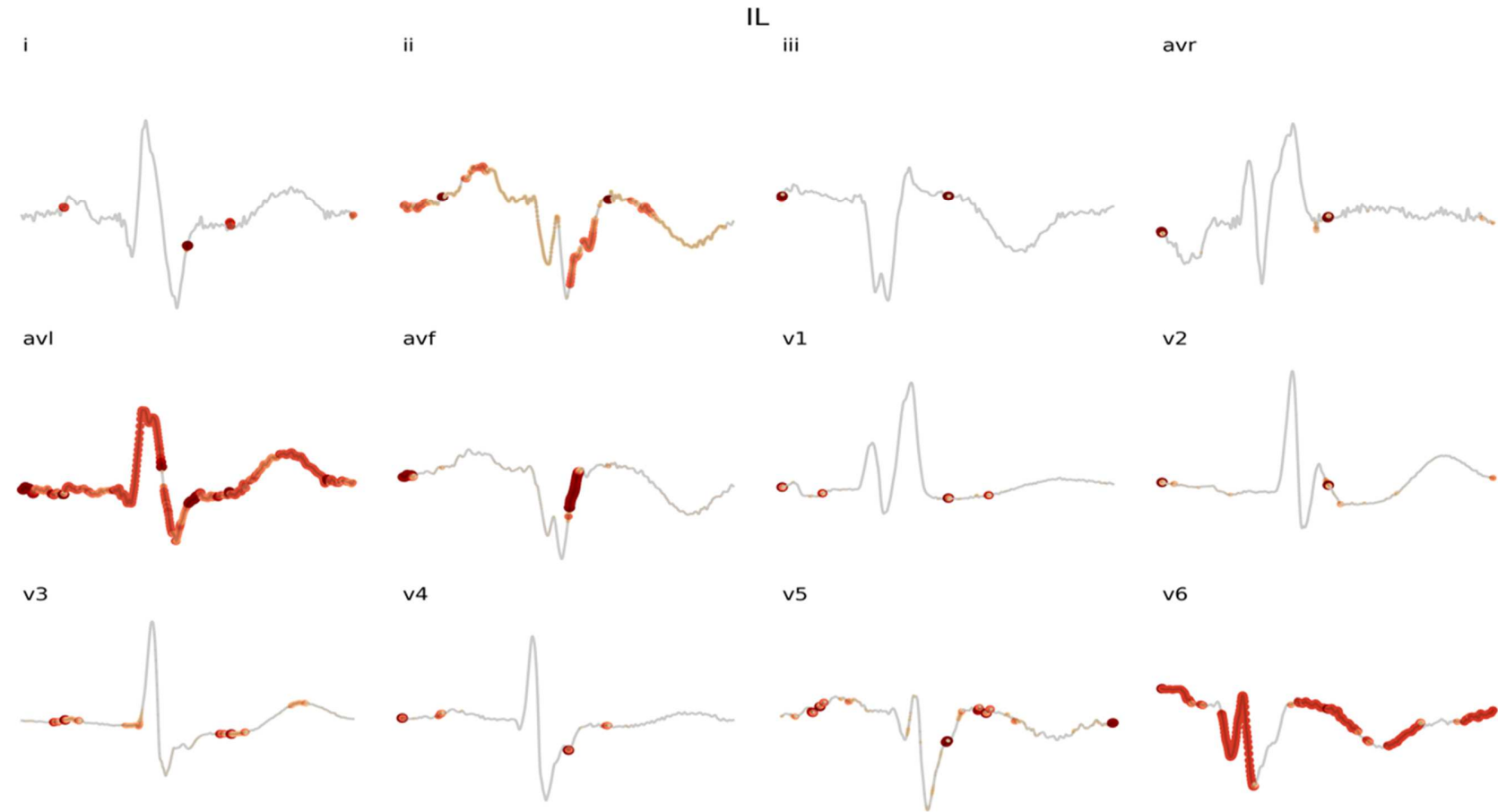


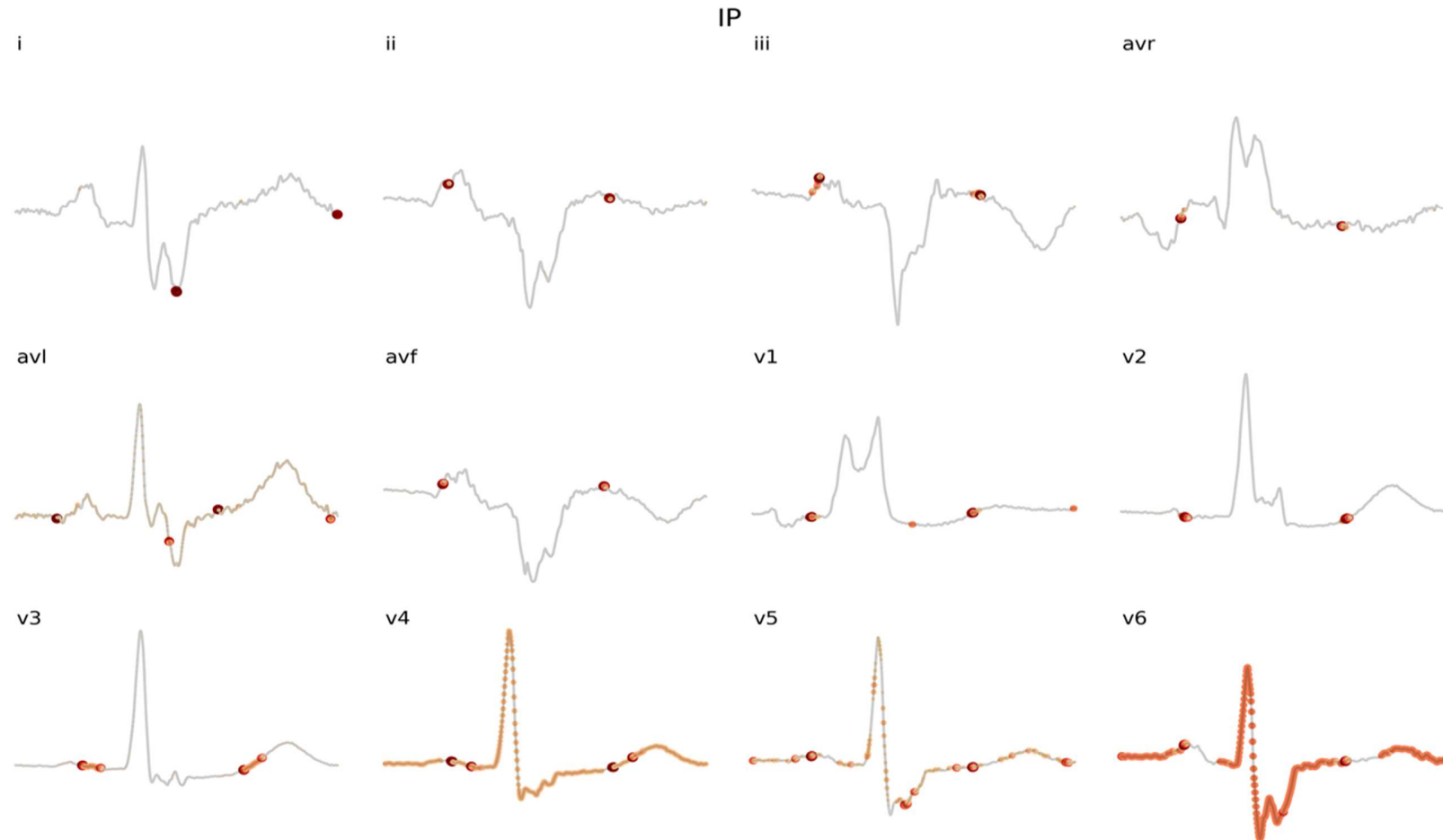


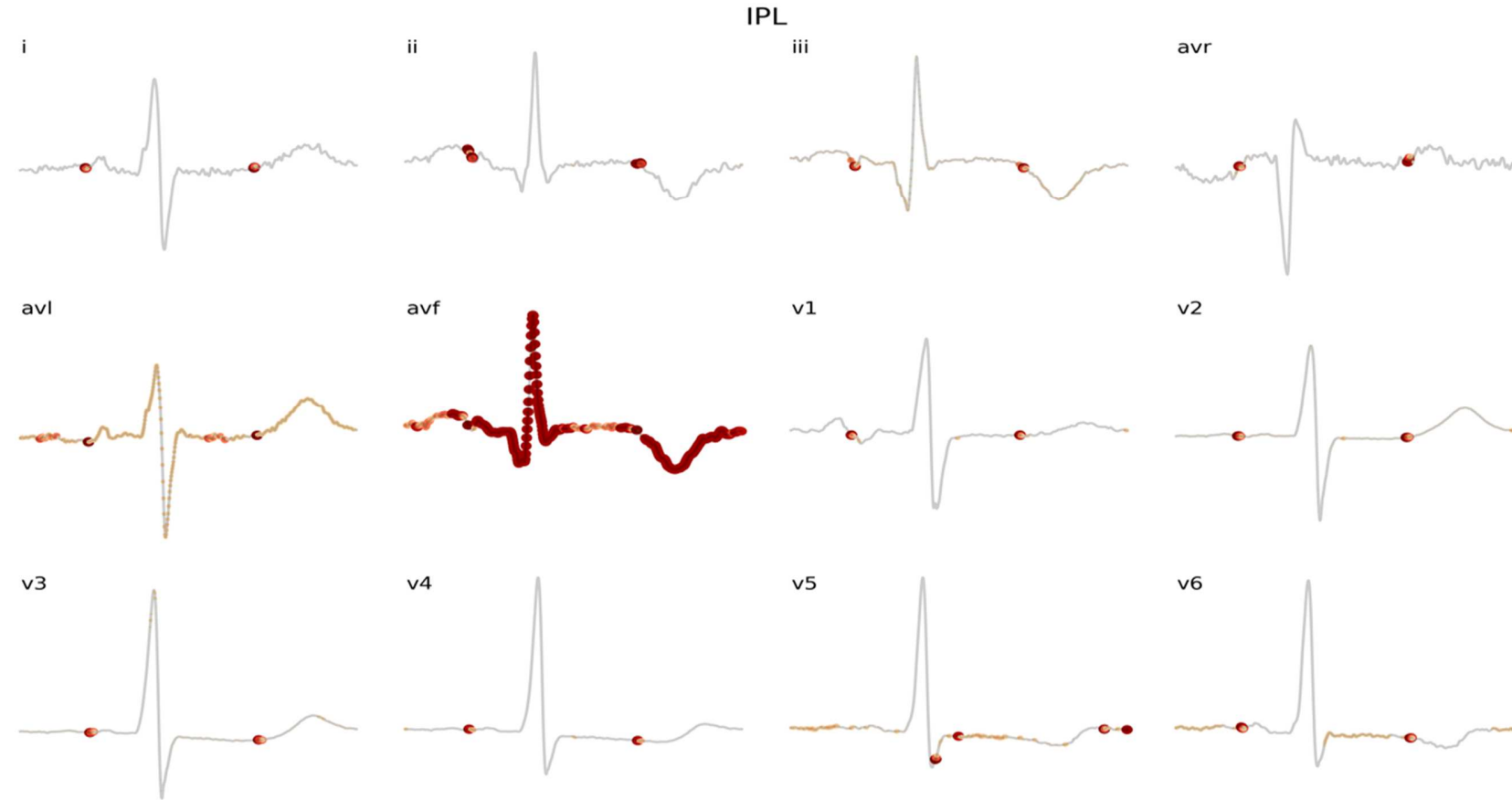


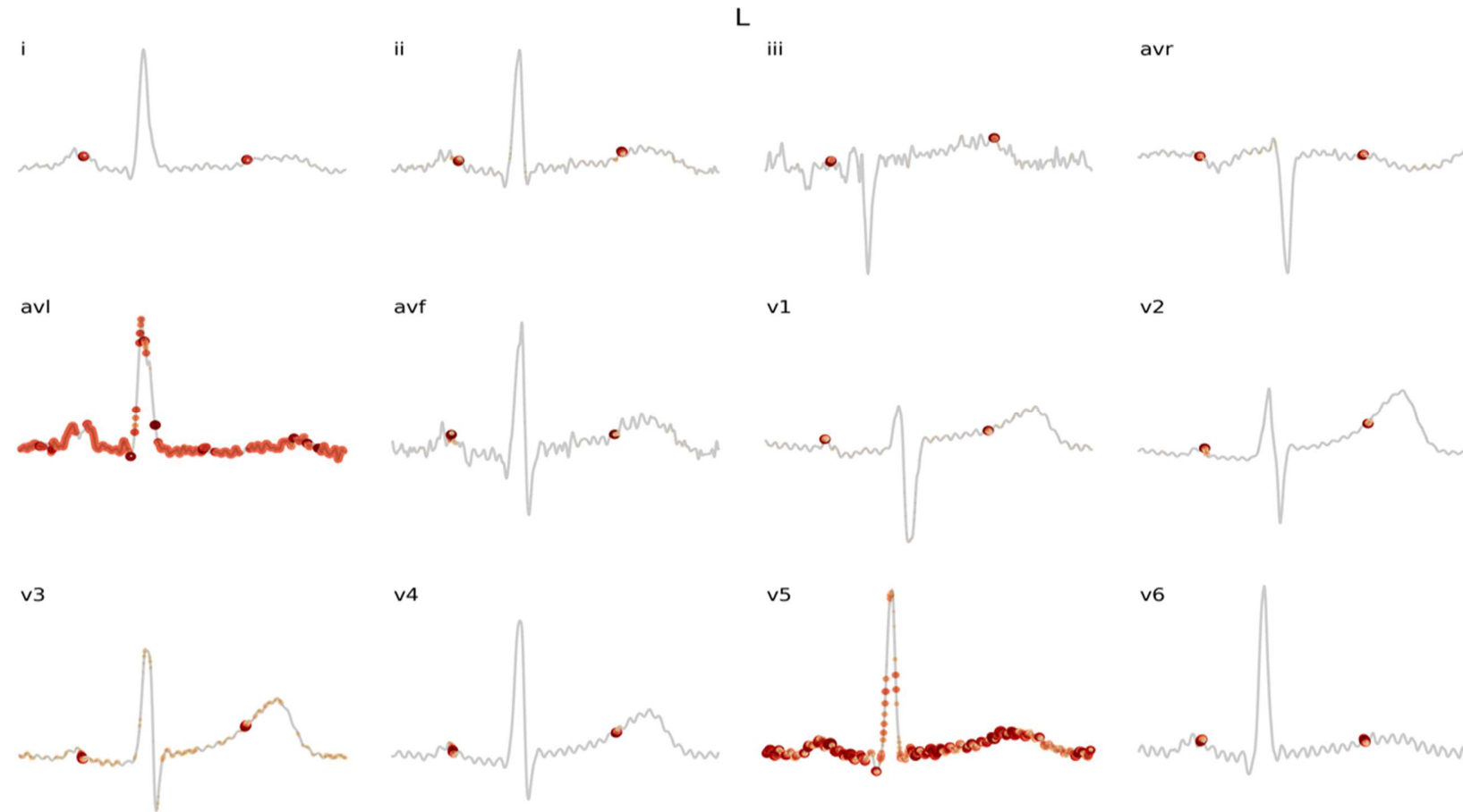


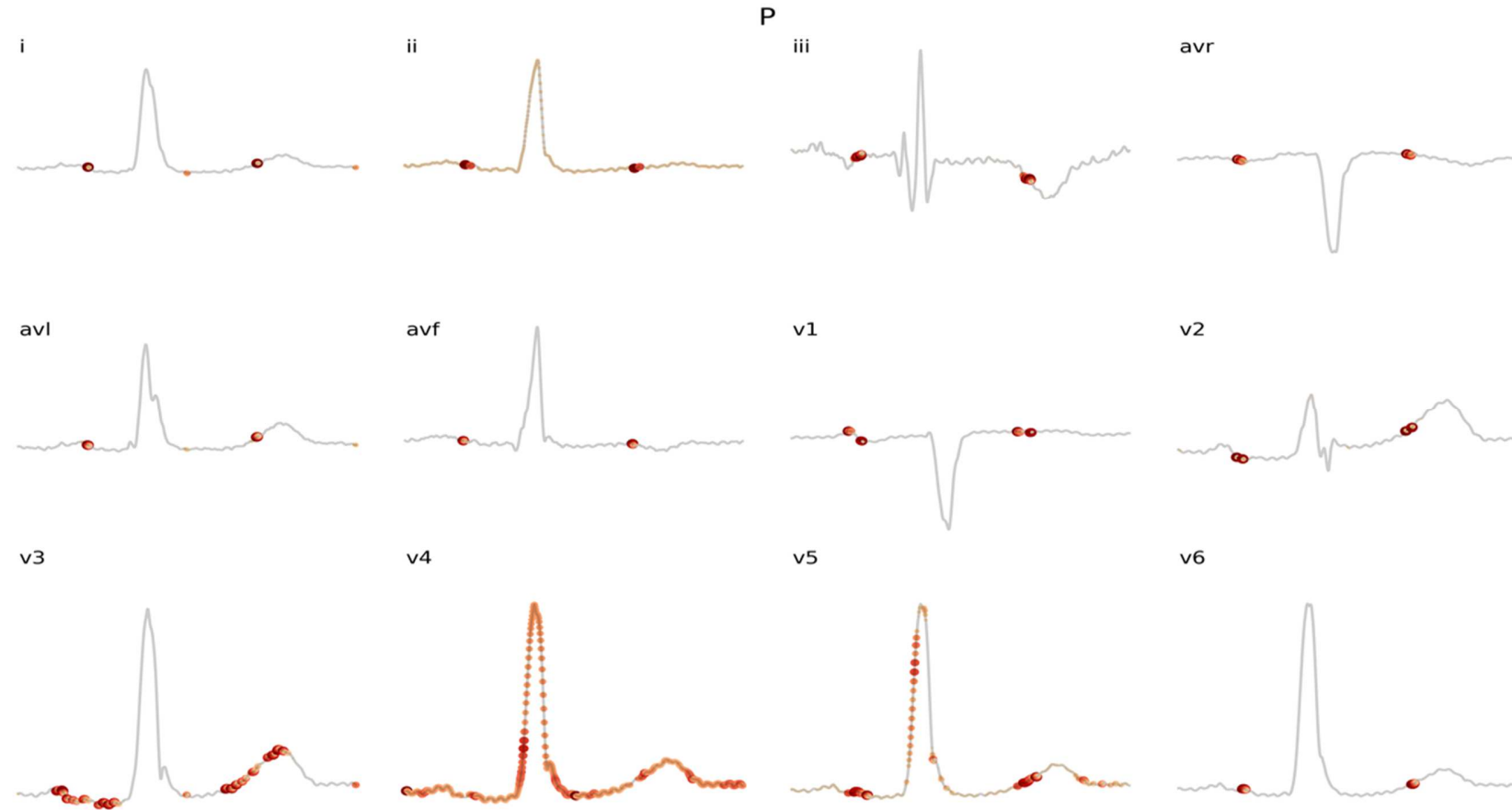












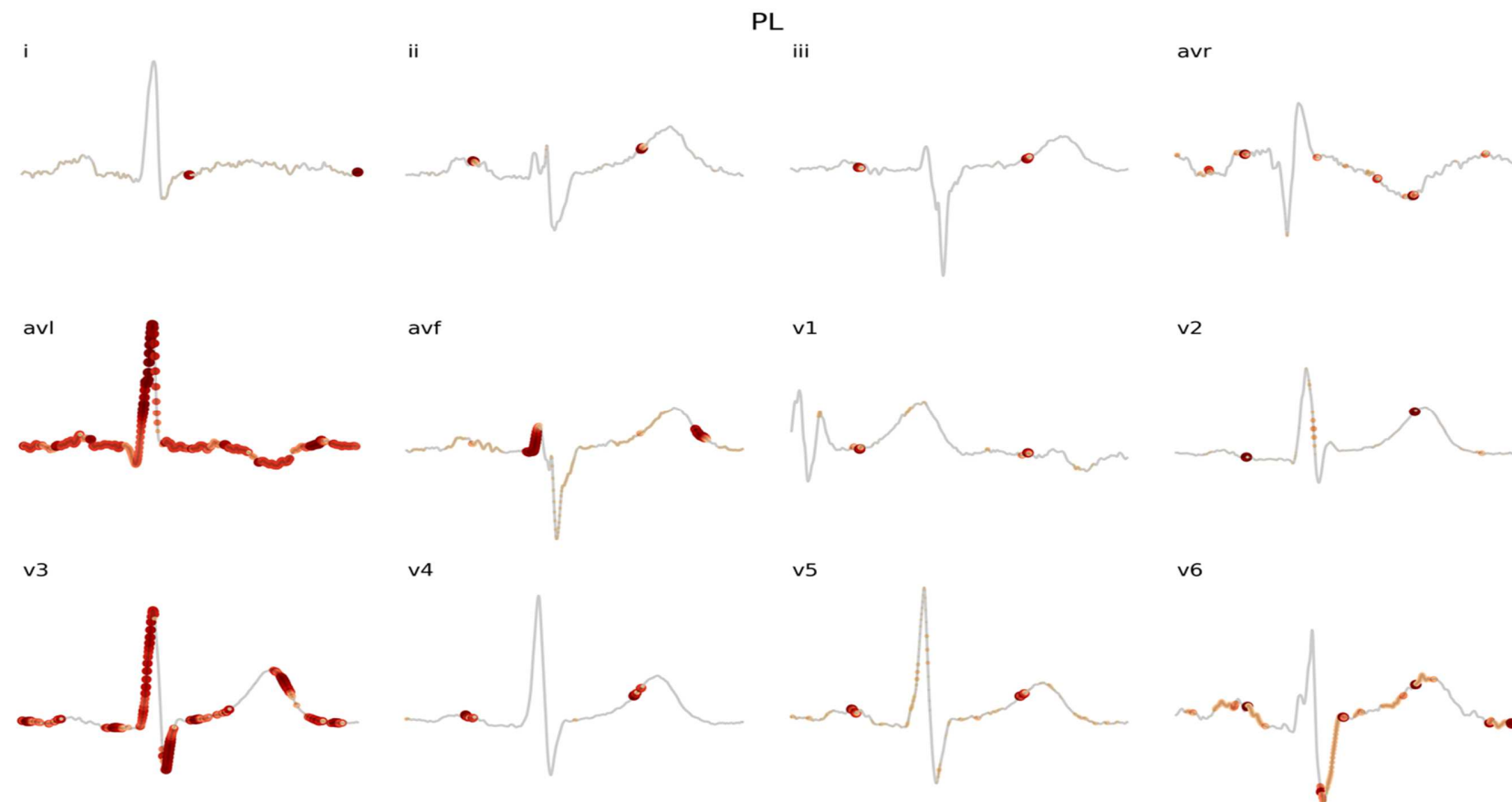
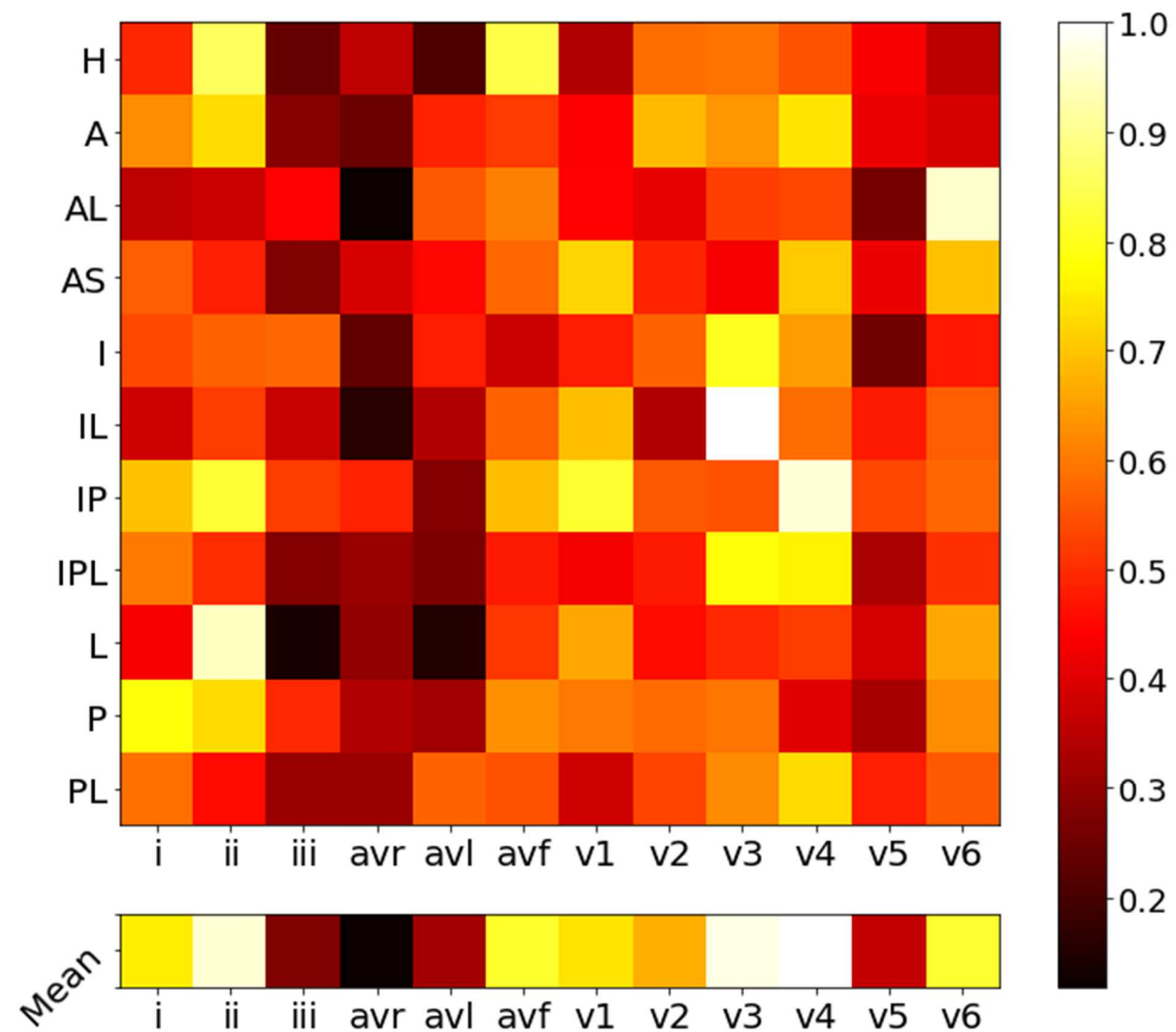


Figure 6. Activation maps of each myocardial infarction class obtained from the Grad-CAM technique (output from CNN model).

Abbreviations for Figures 5 and 6: Anterior, A; anterior lateral, AL; anterior septal, AS; healthy, H; inferior, I; inferior lateral, IL; inferior posterior, IP; inferior posterior lateral, IPL; lateral, L; posterior, P; posterior lateral, PL.



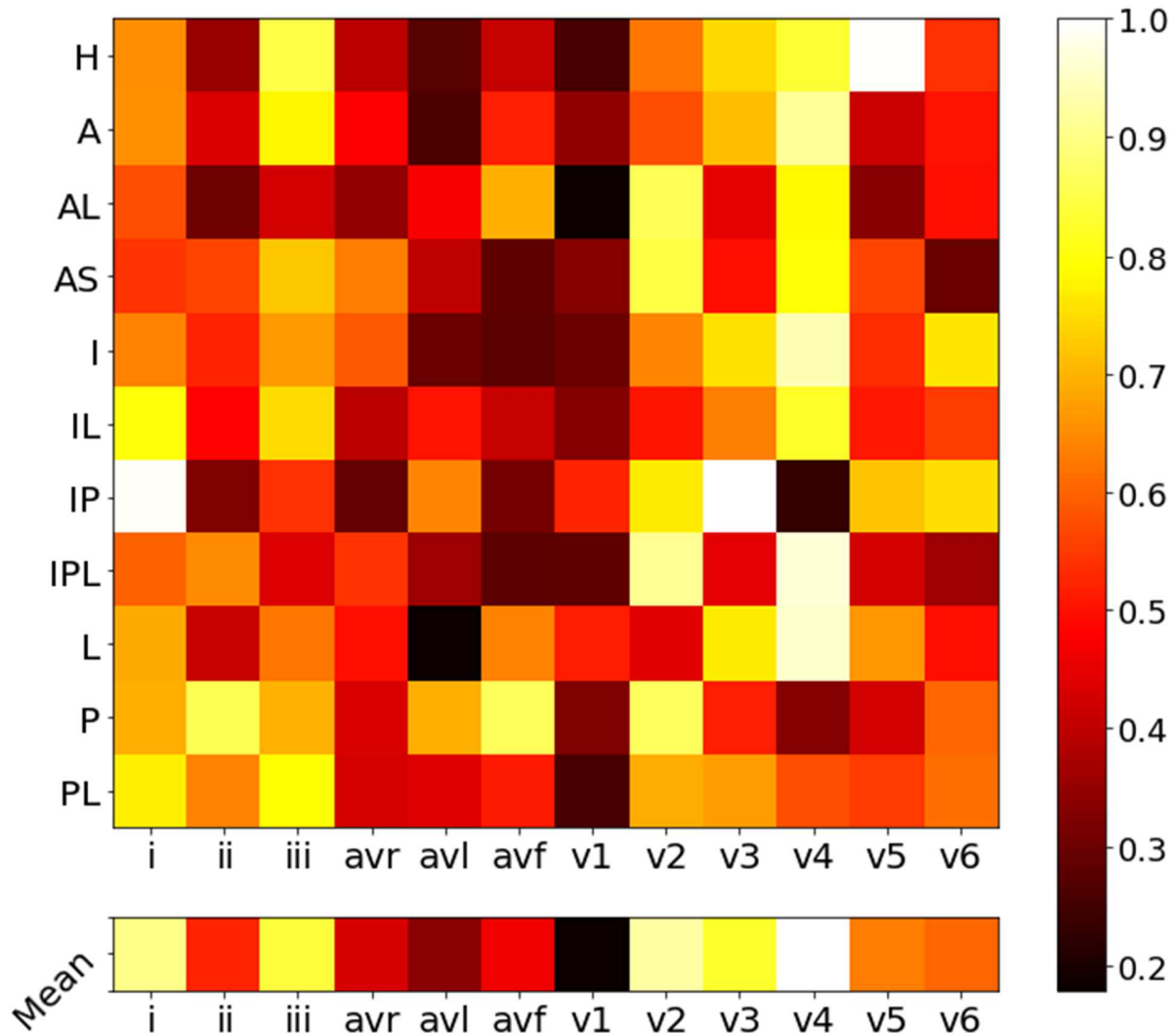


Figure 7. Heat maps of individual lead activations for all myocardial infarction and healthy classes in the DenseNet model (top) and CNN model (bottom). Anterior, A; anterior lateral, AL; anterior septal, AS; healthy, H; inferior, I; inferior lateral, IL; inferior posterior, IP; inferior posterior lateral, IPL; lateral, L; posterior, P; posterior lateral, PL.

Experimental results

For the ECG output from the DenseNet model (Figure 4), P and T waves were generally activated in all leads for detection of anterior MI; P and T waves were most activated in Lead II and P, QRS and T waves in Lead V5 for detection of anterior lateral MI; P and T waves were generally activated in all leads for detection of healthy class; P and T waves were most activated in Lead II and QRS complex in Lead V5 for detection of anterior septal MI; P and T waves were most activated in Lead 2 and P and T waves in Lead V2 for detection of inferior MI; ST segment was most activated in Lead aVF for detection of inferior lateral MI; P, QRS and T waves are the most activated in Lead II for detection of inferior posterior MI; P and T waves were generally activated in all leads for detection of inferior posterior lateral MI; P and T waves were most activated in Lead II for the detection of lateral MI; P, QRS and T waves were most activated in Lead V2 and P, RS and T waves in Lead V5 for detection of posterior MI; QRS complex was most activated in Lead aVR for the detection of posterior lateral MI. For the ECG output from the CNN model (Figure 5), P, QRS and T waves are most activated in Lead II and P and T waves in Lead V6 for detection of anterior MI; P, QRS and T waves were most activated in Leads aVR and V5 for detection of anterior lateral MI; P and T waves were most activated in Lead V5 for detection of anterior septal MI; P and T waves were most activated in Lead aVL for detection of healthy class; P, QRS and T waves are most activated in Lead aVL for detection of inferior MI; P, QRS and T waves are most activated in Lead aVL for detection of inferior lateral MI; P, QRS and T waves were most activated in Lead V6 for detection of inferior posterior MI; P, QRS and T waves were most activated in Lead aVF for detection of inferior posterior lateral MI; P, QRS and T waves were most activated in Leads aVL and V5 for detection of lateral MI; P, QRS and T waves were most activated in Lead V4 for detection of posterior MI; P, QRS and T waves were most activated in Lead aVL and PR and ST segments in Lead V3 for detection of posterior lateral MI. From Figure 6, it is observed that Lead V4 was the most activated lead in influencing the DenseNet and CNN models for the classification of MI and healthy classes.

The advantages and disadvantages of the study are listed below.

Advantages:

1. ECG data comprising all 12 leads were used in this study, while in the related studies, most authors had used only one or a few leads for the classification.
2. ECG data containing all 10 MI classes in the PTB database were used in this study, while in the related studies, some authors had studied only a subset of the 10 MI classes for the classification.
3. Both DenseNet and CNN models attained good classification performance.
4. The developed DenseNet has low computational complexity and has the potential to be applied in the clinical setting for rapid triage of MI.
5. This is the only study that has mapped the classification decision of deep models to specific ECG leads and locations on the ECG signals classifying healthy and ten classes of MI, thereby providing some level of explainability that clinicians can relate to.

Disadvantage(s):

1. The dataset used in this study is imbalanced.
2. A public database has been used in this study instead of authentic hospital data.

8. Conclusion

Of various cardiovascular diseases, MI accounts for the most deaths globally. In acute MI, accurate ECG diagnosis is important for timely intervention in the emergency setting. Machine learning is increasingly being explored for ECG diagnosis of cardiovascular diseases. In this study, we have developed DenseNet and CNN models for the classification of healthy subjects and patients with 10 classes of MI based on the location of myocardial involvement. After pre-processing, the R peaks of individual lead signals of 12-lead ECGs were detected to extract the beats (each beat was composed of sampled data from all 12 leads), which were then input to the DenseNet and CNN models. While both DenseNet and CNN models performed well with high classification performance, DenseNet is the preferred model due to its low computational complexity and feature reusability. The Grad-CAM technique was subsequently applied to the outputs of both models to explain the decisions made by the respective models. The specific ECG

leads and portions of the ECG waves most influential for the detection of each MI and healthy class were visualized. Overall, Lead V4 was the most activated lead with the most influence on the classification in both DenseNet and CNN models. Furthermore, the different leads and parts of signal that get activated for each class have also been established through this study. This is the first study to report features that influenced the classification decisions of deep models for multiclass classification of MI and healthy ECGs. Hence this study is crucial and contributes significantly to the medical field as this offers some level of explainability of the inner workings of the deep models that clinicians may relate to. Thus, developed models combined with Grad-CAM are more likely to garner clinical acceptance and can be used to triage MI in hospitals and remote out-of-hospital settings.

9. References

- [1] L. Ibrahim, M. Mesinovic, K. W. Yang, and M. A. Eid, "Explainable Prediction of Acute Myocardial Infarction using Machine Learning and Shapley Values," *IEEE Access*, vol. 8, 2020.
- [2] L. J. Laslett *et al.*, "The Worldwide Environment of Cardiovascular Disease: Prevalence, Diagnosis, Therapy, and Policy Issues: A Report From the American College of Cardiology," *J. Am. Coll. Cardiol.*, vol. 60, no. 25, Supplement, pp. S1–S49, 2012.
- [3] E. J. Benjamin *et al.*, *Heart Disease and Stroke Statistics-2019 Update: A Report From the American Heart Association*, vol. 139, no. 10. 2019.
- [4] M. Bęćkowski, "Acute coronary syndromes in young women - the scale of the problem and the associated risks," *Kardiochirurgia i torakochirurgia Pol. = Polish J. cardio-thoracic Surg.*, vol. 12, no. 2, pp. 134–138, Jun. 2015.
- [5] W. Zhang *et al.*, "Interpretable Detection and Location of Myocardial Infarction Based on Ventricular Fusion Rule Features," *J. Healthc. Eng.*, vol. 2021, 2021.
- [6] V. Jahmunah, E. Y. K. Ng, T. R. San, and U. R. Acharya, "Automated detection of coronary artery disease, myocardial infarction and congestive heart failure using GaborCNN model with ECG signals," *Comput. Biol. Med.*, vol. 134, p. 104457, 2021.
- [7] J. L. Anderson and D. A. Morrow, "Acute Myocardial Infarction," *N. Engl. J. Med.*, vol. 376 21, pp. 2053–2064, 2017.
- [8] P. Linardatos, V. Papastefanopoulos, and S. Kotsiantis, "Explainable ai: A review of machine learning interpretability methods," *Entropy*, vol. 23, no. 1, pp. 1–45, 2021.
- [9] A. Ullah, S. U. Rehman, S. Tu, R. M. Mehmood, Fawad, and M. Ehatisham-Ul-haq, "A hybrid deep CNN model for abnormal arrhythmia detection based on cardiac ECG signal," *Sensors (Switzerland)*, vol. 21, no. 3, pp. 1–13, 2021.
- [10] Z. Ebrahimi, M. Loni, M. Daneshtalab, and A. Gharehbaghi, "A review on deep learning methods for ECG arrhythmia classification," *Expert Syst. with Appl. X*, vol. 7, p. 100033, 2020.
- [11] J. Li, Y. Si, T. Xu, and S. Jiang, "Deep Convolutional Neural Network Based ECG Classification System Using Information Fusion and One-Hot Encoding Techniques," *Math. Probl. Eng.*, vol. 2018, 2018.
- [12] V. Jahmunah, E. Y. K. Ng, T. R. San, and U. R. Acharya, "Automated detection of coronary artery disease, myocardial infarction and congestive heart failure using GaborCNN model with ECG signals," *Comput. Biol. Med.*, vol. 134, no. February, 2021.
- [13] D. C. K. Soh, E. Y. K. Ng, V. Jahmunah, S. L. Oh, R. S. Tan, and U. R. Acharya, "Automated diagnostic tool for hypertension using convolutional neural network," *Comput. Biol. Med.*, vol. 126, p. 103999, 2020.
- [14] A. L. Goldberger *et al.*, "PhysioBank, PhysioToolkit, and PhysioNet , " *Circulation*, vol. 101, no. 23, pp. e215–e220, Jun. 2000.
- [15] R. J. Martis, U. R. Acharya, and C. M. Lim, "ECG beat classification using PCA, LDA, ICA and Discrete Wavelet Transform," *Biomed. Signal Process. Control.*, vol. 8, pp. 437–448, 2013.
- [16] J. Pan and W. J. Tompkins, "A Real-Time QRS Detection Algorithm," *IEEE Trans. Biomed.*

- Eng.*, vol. BME-32, no. 3, pp. 230–236, 1985.
- [17] G. E. Hinton and R. R. Salakhutdinov, "Reducing the dimensionality of data with neural networks," *Science*, vol. 313, no. 5786, p. 504, 2006.
 - [18] A. Alekseev and A. Bobe, "GaborNet: Gabor filters with learnable parameters in deep convolutional neural network," *2019 Int. Conf. Eng. Telecommun. Ent* 2019, 2019.
 - [19] L. Zhuo, B. Zhang, C. Chen, Q. Ye, J. Liu, and D. Doermann, "Calibrated stochastic gradient descent for convolutional neural networks," *33rd AAAI Conf. Artif. Intell. AAAI 2019, 31st Innov. Appl. Artif. Intell. Conf. IAAI 2019 9th AAAI Symp. Educ. Adv. Artif. Intell. EAAI 2019*, pp. 9348–9355, 2019.
 - [20] G. Huang and K. Q. Weinberger, "Densely Connected Convolutional Networks."
 - [21] D. P. Kingma and J. L. Ba, "Adam: A method for stochastic optimization," *3rd Int. Conf. Learn. Represent. ICLR 2015 - Conf. Track Proc.*, pp. 1–15, 2015.
 - [22] M. Jafari *et al.*, "FU-Net: Multi-class Image Segmentation Using Feedback Weighted U-Net," in *Lecture Notes in Computer Science (including subseries Lecture Notes in Artificial Intelligence and Lecture Notes in Bioinformatics)*, 2019.
 - [23] W. Liu, Q. Huang, S. Chang, H. Wang, and J. He, "Multiple-feature-branch convolutional neural network for myocardial infarction diagnosis using electrocardiogram," *Biomed. Signal Process. Control*, vol. 45, pp. 22–32, 2018.
 - [24] N. Liu, L. Wang, Q. Chang, Y. Xing, and X. Zhou, "A Simple and Effective Method for Detecting Myocardial Infarction Based on Deep Convolutional Neural Network," *J. Med. Imaging Heal. Informatics*, vol. 8, no. 7, pp. 1508–1512, 2018.
 - [25] U. B. Baloglu, M. Talo, O. Yildirim, R. S. Tan, and U. R. Acharya, "Classification of myocardial infarction with multi-lead ECG signals and deep CNN," *Pattern Recognit. Lett.*, vol. 122, pp. 23–30, 2019.
 - [26] W. Liu, F. Wang, Q. Huang, S. Chang, H. Wang, and J. He, "MFB-CBRNN: A Hybrid Network for MI Detection Using 12-Lead ECGs," *IEEE J. Biomed. Heal. Informatics*, vol. 24, no. 2, pp. 503–514, 2020.
 - [27] L. Fu, B. Lu, B. Nie, Z. Peng, H. Liu, and X. Pi, "Hybrid network with attention mechanism for detection and location of myocardial infarction based on 12-lead electrocardiogram signals," *Sensors (Switzerland)*, vol. 20, no. 4, 2020.
 - [28] K. Jafarian, V. Vahdat, S. Salehi, and M. Mobin, "Automating detection and localization of myocardial infarction using shallow and end-to-end deep neural networks," *Appl. Soft Comput. J.*, vol. 93, 2020.
 - [29] J. Zhang *et al.*, "Automated detection and localization of myocardial infarction with staked sparse autoencoder and treebagger," *IEEE Access*, vol. 7, no. June, pp. 70634–70642, 2019.
 - [30] R. K. Tripathy, A. Bhattacharyya, and R. B. Pachori, "A Novel Approach for Detection of Myocardial Infarction from ECG Signals of Multiple Electrodes," *IEEE Sens. J.*, vol. 19, no. 12, pp. 4509–4517, 2019.
 - [31] C. Han and L. Shi, "ML-ResNet: A novel network to detect and locate myocardial infarction using 12 leads ECG," *Comput. Methods Programs Biomed.*, vol. 185, p. 105138, 2020.
 - [32] U. R. Acharya, H. Fujita, S. L. Oh, Y. Hagiwara, J. H. Tan, and M. Adam, "Application of

- deep convolutional neural network for automated detection of myocardial infarction using ECG signals," *Inf. Sci. (Ny.)*, vol. 415–416, pp. 190–198, 2017.
- [33] T. Reasat and C. Shahnaz, "Detection of inferior myocardial infarction using shallow convolutional neural networks," *5th IEEE Reg. 10 Humanit. Technol. Conf. 2017, R10-HTC 2017*, vol. 2018-Janua, no. Imi, pp. 718–721, 2018.
- [34] W. Liu *et al.*, "Real-Time Multilead Convolutional Neural Network for Myocardial Infarction Detection," *IEEE J. Biomed. Heal. Informatics*, vol. 22, no. 5, pp. 1434–1444, 2018.
- [35] H. W. Lui and K. L. Chow, "Multiclass classification of myocardial infarction with convolutional and recurrent neural networks for portable ECG devices," *Informatics Med. Unlocked*, vol. 13, no. June, pp. 26–33, 2018.
- [36] K. Feng, X. Pi, H. Liu, and K. Sun, "Myocardial infarction classification based on convolutional neural network and recurrent neural network," *Appl. Sci.*, vol. 9, no. 9, pp. 1–12, 2019.
- [37] K. Manimekalai, "Deep Learning Methods in Classification of Myocardial Infarction by employing ECG Signals," *Indian J. Sci. Technol.*, vol. 13, no. 28, pp. 2823–2832, 2020.
- [38] J. Jian *et al.*, "Detection of Myocardial Infarction Using ECG and Multi-Scale Feature Concatenate," *Sensors*, vol. 21, 2021.
- [39] A. Holzinger, C. Biemann, C. S. Pattichis, and D. Kell, "What do we need to build explainable AI systems for the medical domain?," no. January 2018, 2017.
- [40] J. K. Kim, S. Jung, J. Park, and S. W. Han, "Arrhythmia detection model using modified DenseNet for comprehensible Grad-CAM visualization," *Biomed. Signal Process. Control*, vol. 73, no. November 2021, 2022.